SOME THREE-DIMENSIONAL ISSUES IN COMPOSITE PIN JOINTS

By

Li Hou

A DISSERTATION

Submitted to
Michigan State University
In partial fulfillment of the requirements
for the degree of

DOCTOR OF PHYLOSOPHY

Department of Mechanical Engineering

2004

ABSTRACT

SOME THREE-DIMENSIONAL ISSUES IN COMPOSITE PIN JOINTS

By

Li Hou

Demands for thick composite plates in mechanical joint structures are booming. Yet still lacking are mechanical joint associated studies related to size scaling effects, especially three-dimensional scaling effects involving thickness scaling. In current research, an original three-dimensional size scaling study was carried out in order to reveal joint load-capacity variation as well as various damage mechanisms caused by size scaling, especially thickness scaling. Woven glass-fabric/phenolic and glass/epoxy composite were included in a double-lap-single-pin joint structure for experimental studies. A previous study was first extended into three-dimensional scaling effect study by combining and comparing thickness scaling effect and in-plane, or two-dimensional, scaling effect. An important geometric ratio H/D, i.e. composite laminate thickness H to fastener hole diameter D, was found to be influential to size scaling effects in many aspects. Later, three technical approaches in meeting out-of-plane constraint requirements, or thickness constraint requirements, of a mechanical joint structure – thickness scaling, bonding technique and bolting technique were compared. Their key roles in local and global damage process were discussed. Finally, a three-dimensional finite element analysis was carried out in order to reveal stress distribution through the thickness direction and its sensitivity to thickness scaling effect. Several commonly-used failure criteria were investigated for suitability on glass/epoxy case. A broadened two-parameter failure theory was also included for discussion.

ACKNOWLEDGMENTS

My sincere gratitude goes to Professor Dahsin Liu (Mechanical Engineering Department, Michigan State University) for constantly guiding and supporting this research. Professor Liu and his previous students' research work initiated this study. And this study could not possibly reach current level without his continuous contribution.

I would like to thank John F. Whalen (Vice President, Fisher Dynamics at ST. Clair Shores, MI) and Peter Rizk (Program Manager, Hydro Automotive Structures at Holland, MI) for encouraging continuous pursue of this study.

I thank my wife, Aijun and my daughter, Aili for their support during this six-year-long project. Aili, now a two-year-old, has in her own way taught me how to be persistent and patient in my research. I would like to acknowledge my parents, Naiwen and Yiai who gave me the opportunities to reach my goals and did that at a great personal sacrifice.

Table of Contents

List of Tables

List of Figures

Chapter 1

Introduction

1.1 Statement of Problem and Literature Review

A. Thick Composite Plate

What we today call composites, or more specifically fiber-reinforced plastics, were first produced five decades ago. Fibers, primarily glass, were first converted into different forms, such as woven-fiber or unidirectional-fiber, which were then impregnated with a plastic matrix resin, e.g. epoxy, into a composite ply. Multiple numbers of composite plies, each possibly at a different orientation, were then stacked together into a composite laminate plate.

Due to their high strength and light weight but high cost, composite materials were initially developed for, yet limited to, aerospace structural applications. Since most composite plates back then were of a much smaller dimension in thickness as compared to other two in-plane dimensions, i.e. length and width, they were generally viewed as thin plates. Accordingly, in-plane mechanical behaviors of composite plates have drawn much more attention than out-of-plane mechanical behaviors, associated with thickness direction, over the past several decades.

Ever since their birth, however, composites have gradually worked their way into a seemingly endless number of applications beyond aerospace industry. Meanwhile, demands for thick-section composite plates, generally defined as thicker than one half inch, are quickly booming. Submarine hull and armored vehicle bodies, for example, demand rigorous mechanical performance requirements in the thickness only thick composite plates could possibly meet. The extension from thin composite plates to thick

ones, however, is not trivial. In fact, it requires careful modifications in many aspects of composite technologies, e.g. manufacturing, testing, analysis and design [1-7].

B. Mechanical Joining Technique

Joining is a secondary process in structure manufacturing. In manufacturing conventional metallic structures, small components are fabricated individually and then assembled to form large sections. Although complex composite structures can be molded in single pieces to simplify manufacturing processes and to reduce assembly cost, they cannot be completely exempted from the joining process. The joining process is especially needed when composite components are to be assembled with components made of dissimilar materials, such as metals.

Both mechanical fastening and adhesive bonding are commonly used in structure assemblies. Each technique has its own advantages and disadvantages in terms of function, cost, etc. Adhesive bonding is privileged for being free from structural discontinuity. In terms of structural strength, however, adhesive bonding is primarily relying on shearing strengths of adherent, adhesion and the bonding between them [8,9]. Also well recognized, shearing strengths are not as promising as the in-plane strengths and shear stress related failures are often catastrophic [10]. Moreover, as components to be assembled in a joined structure become thicker, substantially increasing bonding areas two-dimensionally and applying complex joining techniques [11-13], such as scarf joints, prove to be only available options. On the other hand, thicker components could be straightforwardly incorporated in a mechanical fastening by increasing fastener size accordingly. As a result, high in-plane strengths of composite materials could be fully taken advantage of and high stress concentrations due to structural discontinuity could be

released. Therefore, in joining thick composite laminates, mechanical fastening technique is superior to the adhesive bonding technique thanks to its three-dimensional nature.

Generally, the parameters affecting the performance of a mechanical joint could be categorized into three groups: (1) Material parameters: fiber type and form (woven fabric, unidirectional, etc.), resin type, fibre orientation, laminate stacking sequence, etc.; (2) Fastener parameters: fastener type (screw, bolt, rivet etc.), fastener size, hole size, tolerance, washer size, clamping force, side lap material and geometry; (3) Design parameters: joint type (single lap, double lap, multiple/single fastener), in-plane geometry (width, length, end distance, hole pattern, etc.), laminate thickness, load direction, loading rate, etc.

C. Size Scaling

Small coupons are usually used in laboratories for material characterizations. Results from small coupon tests are then used for design of large structures. However, small coupons do not always behave the same as large structures made of an identical material [14-18]. The difference of behaviors due to size variation is usually called "size scaling effects". Some investigations regarding the performance of composite materials at different scales have been reported [16-18]. It has been concluded that scaling effect should be carefully examined in material characterization and structural designs.

In an adequate design of mechanical joint structure, moreover, size scaling effect is complicated and can be categorized into in-plane scaling, thickness scaling and three-dimensional scaling. As a matter of fact, in-plane scaling is based on the presumption of uniform material properties and stress distribution in the thickness direction and has been more thoroughly studied; thickness scaling did not draw much attention until recently

when broad thick composite plate application became reality. Research on three-dimensional scaling is even more scarce.

In studying in-plane scaling, thin composite laminates without notches [18] and with notches [16] were investigated. The strengths of composite laminates were found to decrease monotonically with the increase of in-plane dimensions. In a two-dimensional study on mechanical fastening, Wang et al [19] reported that the bearing strength had a first-decrease-then-increase change as the in-plane dimensions increased.

Thickness also plays an important role in composite size scaling [1, 3, 6, 17]. In fact, there are some unique concerns in scaling the thickness of composite laminates. Unlike scaling the thickness of conventional metals, there exist at least two different approaches in scaling thicknesses of composite laminates, so-called sub-laminate scaling and ply-thickness scaling, each meeting different design purposes. Various stacking sequences also result into different failure phenomena and mechanisms [21]. Also, limited by the immaturity of manufacture technology, thick composites unavoidably contain residual stresses to some extent [21-24]. As a result, material property variation would become noticeable not only between thin and thick composite plates, but also within a thick composite plate itself, through the thickness direction between inner and outer plies. Moreover, geometry-induced variations including non-uniform stress distributions through laminate thickness, specifically as in mechanical joining structure [25-27], render the study very complicated.

In a previous study [28] regarding to thickness scaling involved in mechanical joint, the thickness effect in composite pin joints was found to be dependent on the ratio of laminate thickness H to hole diameter D, i.e. H/D. If the H/D ratio is smaller than 1.0,

the pin joint has a relatively small thickness but a relatively large hole. On the contrary, if the H/D ratio is greater than 1.0, the pin joint has a relatively large thickness but a relatively small hole. As the H/D ratio changes from smaller than 1.0 to greater than 1.0, both the types of the load-displacement curve and the strengths of the composite joints change significantly due to the change of the contact condition between the pins and the composites. Joint configurations with ratios of H/D close to one were found to be more efficient in joint performance.

D. Investigation Techniques

Many analytical studies concerning mechanical fastening were presented and most of them were based on two-dimensional assumptions. However, as mentioned by Oplinger [25], two-dimensional studies unavoidably ignored the details of the stress distribution through the thickness of the fasteners. Nelson, Bunin and Hart-Smith [26] also presented some important insights into the effects of thickness on fastener bending. The importance of using three-dimensional techniques in studying mechanical fastening was also recognized by other researchers [27, 29-31]. According to Chen, Lee and Yeh [28], the bolt elasticity had a tendency to change the stress distribution through the laminate thickness. Ireman [27] found that bending of the bolt created a non-uniform contact stress distribution between the bolt and the hole. An investigation based on a three-dimensional spline variational technique was conducted by Iarve and Schaff [31] to analyze the interlaminar stresses in a composite fastener.

Among the very few studies based on three-dimensional analysis, the interlaminar stresses between different layers were often not examined thoroughly. Shokrieh and Lessard [32] studied a pin-joint structure with radial displacement boundary conditions.

Stress singularities were reported at the interface between layers with different ply orientations on the free edges. However, the contact stress and friction between the pin and the plate were not considered in their study.

Many studies [33-36] were focused on predicting the strength of joint structures solely based on the stress distribution on the hole surface. Their studies belonged to the category of so-called "one-parameter failure theory". Stresses, strain or distortional energy results right on the hole surface were input into a failure criterion, e.g. maximum stress criterion, to predict the failure of entire joint structure. The one-parameter failure theory was simple to apply but did not account for the localized material response near the hole. Hart-Smith [37] experimentally reported that prior to the entire structure failure localized damage could occur near the hole, instead of right on the hole surface. As a result, one-parameter failure theory generally underestimated the strength of composite joints.

The idea of two-parameter failure theory was taken from Whitney-Nuismer's work [38], which was originally focused on hole size effects. A characteristic dimension, which was normally a certain distance away from the hole in the laminate plane, was required in both point stress and average stress failure theory. The characteristic dimension was considered as a material property in early studies. Later investigations [39.40], however, proved that it was dependent upon laminate quality and type of load. Furthermore, it was concluded that the predicted failure loads were quite sensitive to the value of the characteristic dimension [39-41] or the shape of the characteristic curve [42]. Thus, the two-parameter failure theory was problem dependant and could not be used straightforwardly.

With the assumption that damage took place in the zones where a failure criterion was satisfied, progressive damage theories were proposed to simulate damage initiation. Besides, with the use of elastic property degradation as a function of the degree of damage, progressive damage theories were further used to simulate damage growth [43-47]. The predicted failure loads were in good agreement with experimental results for open holes subjected to compression and tension, by Chang and Lessard [48] and by Chang, Liu and Chang [49], respectively. However, the good experimental correlation can be partially due to the fact that the authors used the value of δ, fibre failure interaction zone introduced by Tsai [50],which best fit with the test data for CFRP. Furthermore, the damage growth used in the compression case [48] was sensitive to the finite element mesh used, so the authors adopted meshes in order to obtain expected damage propagation for each lay-up. This procedure also disabled the generalization of the model for lay-ups and geometries in which damage propagation was difficult to predict. For loaded holes [51], no improvement in accuracy was found in predicting joint strengths with or without the progressive damage models [42, 52].

Also as an open hole study [53], Tan's approach neglected the different effects of different micro-mechanical failure types on the stiffness degradation of a lamina as used by Chang [44]. The stiffness degradation was represented by factors assumed and lamina material properties, E_{11}, E_{22} and G_{12}, were reduced by the product of their initial values with the corresponding factor. Close correlation with experimental data was achieved for several lay-ups in terms of strengths. However, it should be noticed that the results were very sensitive to the values of the degradation factors assumed.

1.2 Objectives and Scopes of Current Study

Studies devoted to size scaling effect in a mechanical joint structure are scarce yet very crucial to an adequate design. Especially, while more and more thick composite plates have been widely practiced in joint systems, scaling effects involving thickness scaling have not drawn as much research attention as they actually deserve. This could be attributed to many factors: thick composite plates are generally expensive; scaling effect theories in composite fields are still lacking; a large variety of failure phenomena compete with each other in a composite material at the same time and their underlying mechanisms have not yet been fully understood; computational simulation of joint structure through thickness is very costly, etc. Nevertheless, research in this area could be rewarding and this study was primarily devoted to size scaling effect, particularly thickness scaling effect, in composite joint system. As regarding to research approaches, experimental study and computational study were both explored intending to provide different perspectives.

As stated before, many parameters affect the performance of a mechanical joint. As a matter of fact, bolt-joint is more commonly practiced in the industry and attracts more research [19, 25, 27, 30, 54-56], as compared with pin-joint. Bolt-joint practice, however, introduces clamping force, another important parameter in the thickness direction other than thickness dimension parameter, and results in a state of intertwining between these two key parameters. A pin joint structure, on the other hand, could single out thickness parameter by simply eliminating the clamping force parameter in a mechanical joint. Since this study was mainly devoted to thickness parameter, pin joint was focused accordingly. Through the entire research, therefore, the joint structure studied was a so-

called "double-lap-single-pin" joint - double side laps and one single pin, assembled with one central composite material lap. For generalization purpose [57-59], woven glass-fabric/phenolic composite and cross-ply glass/epoxy composite were both included in the study.

1.3 Organization of Following Chapters

Firstly, a previous study [28] was extended into a three-dimensional scaling effect study by combining and comparing thickness scaling effect and in-plane scaling effect. A woven glass-fabric/phenolic composite was first selected for study. Based on four different thicknesses and seven different hole diameters, total nine composite joining configurations were prepared. The nine configurations were organized into three groups with different H/D ratios (thickness vs. hole diameter). Strength results as well as damage modes within these groups were compared in order to reveal size scaling effects. Effects due to variation of outer-lap stiffness and pin hardness were also discussed. Experimental results were included in Chapter 2.

Later in Chapter 3, three-dimensional scaling effect study was extended to Glass/epoxy composite laminates. In addition, this part of the study also explored three different technical approaches in meeting out-of-plane requirements of a mechanical joint structure – thickness scaling, bonding technique and bolting technique. Key factors related to constraints in the thickness direction, namely composite thickness, bonding strength through laminate thickness and clamping force from bolting, were compared and their key roles in damage process were discussed. Beyond that, effects due to variation of pin-hole clearances and loading rates were also studied.

Chapter 4 was aimed at gaining more insights into thickness-involved effects in a joint structure by using the aid of finite element analysis method - a computational analysis method. When a glass/epoxy composite joint was subjected to a load comparable to its load capacity, stress distributions around damage susceptible areas were presented in detail attributed to a fine three-dimensional meshing. Stress variation through the thickness direction was studied and its sensitivity to thickness scaling effect was also studied. Suitability of several commonly-used failure criteria was investigated in this special case. A broadened two-parameter failure theory was also included for discussion.

Chapter 5 drew several conclusions of this study and laid out some recommendations for future studies.

Chapter 2

Three-dimensional Size Effects in Composite Pin Joints

2. 1 Introduction

Joining is a secondary process for structure manufacturing. For conventional metallic structures, small components are fabricated individually first and then assembled to form large sections. Although many polymer matrix composite structures can be molded in single pieces to simplify manufacturing process and to reduce assembly cost, they cannot be completely exempted from joining process. The joining process is especially necessary when a polymer composite component is to be joined with a component made of a dissimilar material such as metal.

Both mechanical fastening and adhesive bonding are commonly used in structure assemblies. Each technique has its own advantages and disadvantages in terms of function and cost. In terms of strength, different techniques also lead to different damage modes and failure strengths. Based on the high in-plane strengths of composite materials, mechanical fastening is commonly performed in assembling composite laminates. However, mechanical fastening can cause high stress concentration due to structural discontinuity. Adhesive bonding, although free from structural discontinuity, is primarily based on the shearing strengths of the adherent, the adhesion and the bonding between them. These shearing strengths are no greater than the in-plane strengths and are limited to the bonding surface, instead of through the thickness. As the joining components become thicker, a much larger bonding area is required, not only to achieve a higher joining strength but also to reduce the high stress concentration around the bonding ends. Since mechanical fastening is actually a three-dimensional technique, it is superior to two-dimensional adhesive bonding in joining thick composite laminates.

Thickness is an important parameter in composite structure analysis and many studies concerning thickness effects have been reported in the literature [1, 3-6]. Although studies of composite mechanical fastening commonly focus on effects due to in-plane configuration, the effects due to thickness should also be adequately considered. As mentioned by Oplinger [25], two-dimensional studies unavoidably ignore the details of the stress distribution through the thickness of the joint. Nelson et al. [26] have provided some important insights into the effect of thickness on fastener bending. The importance of using a three-dimensional technique in the analysis of mechanical fastening has also been recognized by other researchers [27, 29, 30]. According to Chen et al. [30], the bolt elasticity has a tendency to change the stress distribution through the laminate thickness. Ireman [27] has found out that bending of the bolt creates a non-uniform contact stress distribution between the bolt and the hole.

In a previous study by Liu et al. [28], the effects of thickness on composite pin joints have been identified as associated with the ratio of laminate thickness to hole diameter, i.e. H/D. Wehn H/D < 1, it implies that the pin joint has a small thickness but a large hole. When H/D > 1, it implies that the pin joint has a large thickness but a small hole. As the H/D ratio changes from less than one to greater than one, both the type of the load-displacement curves and the joining strengths change significantly due to the change of contact between the pins and the composites. The objective of the present study is to identify the effects of three-dimensional scaling (thickness scaling as well as in-plane scaling) on the behavior of composite pin joints.

2. 2 Experimental Methods

A. Composite Material

The composite material used in the study was made of S-2 glass fabrics and a phenolic matrix, namely a glass-fabric/phenolic composite. Since the glass fabrics were of plane weave, each piece of fabric could be viewed as a (0/90) cross-ply unit. In preparing composite laminates, an angle of 45° was imposed in laying up consecutive plies of fabric, resulting in quasi-isotropic laminates $[(0/90)/(45/-45)]_{ns}$. This stacking sequence could be considered as a sublaminate mode of scaling in laminate thickness as the building block [(0/90)/(45/-45)]. Composite laminates of 8-ply (n=2), 24-ply (n=6), 40-ply (n=10) and 80-ply (n=20) were prepared in the study. Thus all laminates tested were quasi-isotropic.

B. Joint Configurations

The 8-ply, 24-ply, 40-ply and 80-ply composite laminates had thicknesses of 1.96, 5.97, 9.40 and 20.42mm, respectively. In order to investigate the effects due to three-dimensional scaling, seven hole sizes were chosen to match the four thicknesses, resulting in nine different joint configurations. The geometric elements of the joints, such as width W, hole diameter D, thickness H and the distance between hole center and specimen end E, and the associated geometric ratios, such as W/D, E/D and H/D, were important parameters in studying mechanical fastening. The geometric elements and ratios of the nine joints were summarized in Table 1. To ensure bearing failure, instead of a net-section or a shear-out failure, all laminates had W/D= 4 and $E/D \geq 2.66$.

For identification purpose, a special notation system based on HXDY has been used where H and D, as defined earlier, represent the thickness and the hole diameter of the

Table 1 – Geometrical elements and geometrical ratios of glass-fabric/phenolic composite central laps.

unit: mm	8-ply	24-ply	40-ply	80-ply
H	1.96	5.97	9.40	20.42
ID	H8D2.77	H24D3.96		
D	2.77	3.96		
W	11.08	15.85		
E	7.48	10.62		
H/D	0.71	1.51		
W/D	4.00	4.00		
E/D	2.70	2.68		
ID	H8D5.16	H24D7.54	H40D6.35	
D	5.16	7.54	6.35	
W	20.33	30.46	20.54	
E	13.73	20.51	17.02	
H/D	0.38	0.79	1.48	
W/D	3.94	4.04	4.00	
E/D	2.66	2.72	2.68	
ID		H24D15.1	H40D12.7	H80D12.7
D		15.09	12.7	12.7
W		60.96	50.80	50.80
E		41.20	34.04	34.04
H/D		0.40	0.74	1.61
W/D		4.04	4.00	4.00
E/D		2.73	2.68	2.68
ID			H40D25.4	**H/D=1.5**
D			25.4	
W			101.6	**H/D=0.75**
E			68.33	
H/D			0.37	
W/D			4.00	
E/D			2.69	**H/D=0.4**

H: laminate thickness
W: laminate width
D: hole diameter
E: distance from hole center to laminate end

joints, respectively, while X and Y are the ply number of the composite laminate and the hole diameter in millimeters (mm), respectively. For example, a composite joint having a thickness of 8-ply (1.96mm) and a hole diameter of 2.77mm is designated as H8D2.77.

C. Three-Dimensional Scaling

Although all composite joints investigated in the study have identical W/D (equal to 4) and similar E/D (greater than 2.66), their H/D ratios are different. Based on the ratio of H/D, the nine joints listed in Table 1 could be divided into three groups. Each group consists of three joints along a diagonal line of Table 1. The three groups had H/D ratios of 0.4, 0.75 and 1.5. The joints with H/D=0.4 and H/D=0.75 have relatively small thicknesses but large hole diameters. The joints with H/D=1.5 have relatively large thicknesses but small hole diameters. Since the joints in each group have identical geometric ratios of W/D, E/D and H/D but different values of geometric elements W, D, H and E, they are of three-dimensional scaling.

D. Dissimilar-Material Assembly

Some experimental results of double-lap-single-pin joints have been reported in a previous study [28]. Both the central laps and the outer laps of the composite joints were made of glass-fabric/phenolic composite, resulting in composite-composite similar-material assemblies. In the present study, a similar double-lap-single-pin joint, as shown in Figure 1, was taken as the experimental model due to the simplicity of this arrangement. However, the central laps were made of the glass-fabric/phenolic composite whereas the outer laps were made of steel, resulting in composite-steel dissimilar-material assemblies. Since various joint configurations with different geometric elements and ratios were investigated, different thicknesses of steel outer laps were required. In the

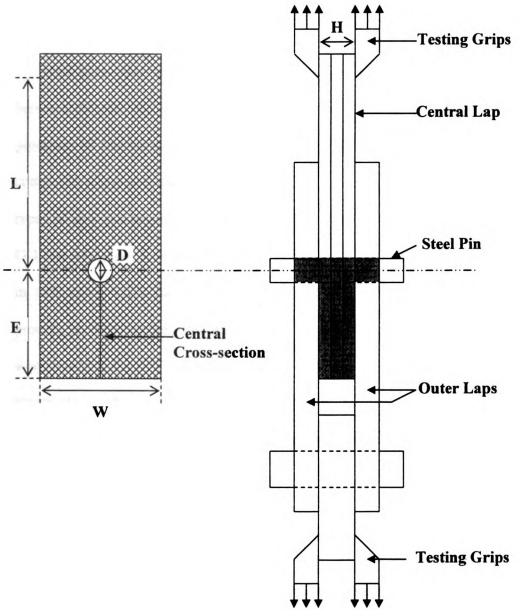

Figure 1 – Schematic diagram of a double-lap-single-pin joint.

study, the thicknesses of the steel outer laps were chosen to be half those of the corresponding composite central laps to ensure the failure of the composite-steel assemblies be dominated by damage to composite central laps. Since steel was stiffer than the composite, the effect of the rigidity of the outer laps on the bearing failure of the composite joints was also a primary concern in the study.

E. Pins with Various Hardnesses

Steel pins were used in the assembly of composite joints. Since the interaction between the pins and the composite central laps played an important role in the failure processes of the composite joints, the effect of pin hardness on the bearing strength of composite joints was also a primary concern in this study of mechanical fastening. Three types of steel pin based on different heat treatment processes were used. They were W-1, O-1 and M-2, based on the AISI classification system. The W-1 pins and O-1 pins were in soft states while the M-2 pins were hardened before applications. The hardening process boosted the hardness of the pins significantly. The hardness indices of the pins were 6.0-13.4 for W-1 pins, 8.5-13.4 for O-1 pins and 63-65 for M-2 pins, based on Rockwell Hardness. The yielding stresses of the pins were proportional to their hardnesses [62, 63]. Consequently, M-2 had the highest yielding stress, followed by O-1, and W-1 had the lowest yielding stress.

2. 3 Experimental Results

A. Load-Displacement Curves

All composite joints were loaded with a constant crosshead rate of 1.27mm/min until bearing failure took place. The obtained load-displacement curves could be divided into two different types: brittle and ductile. If a load-displacement curve had an almost linear

relation until an abrupt loss in load of at least 10%, it was called a brittle-type curve. If, however, the displacement of a curve increased smoothly, not necessarily linearly, with the load and there was no sudden load loss in the curve, the load-displacement curve was called a ductile-type curve. Figure 2(a) shows an example of a brittle-type curve for an H8D2.77 joint while Figure 2(b) shows an example of a ductile-type curve for an H80D12.7 joint. Table 2 summarizes the types of load-displacement curves of all joints based on W-1 pins. The type of the load-displacement curve of a joint was dependent on the H/D ratio of the joint. According to the table, all the joints in the groups with H/D=0.4 and H/D=0.75 had brittle-type curves while all the joints in the group of H/D=1.5 had ductile-type curves.

As hypothesized in a previous study [28], the ductile-type curves were mainly attributed to pin bending. The joints in the group of H/D=1.5 had relatively small hole diameters but large laminate thicknesses. The combination of a small-diameter pin and a large-thickness composite resulted in a non-uniform pin-hole contact through the laminate thickness. A similar result was also reported by Ireman [27] based on three-dimensional finite element analysis. More specifically, the contact between the pin and the composite laminate of the central lap was tighter at the vicinity near the laminate surfaces whereas it was looser at the vicinity near the laminate mid-plane, as shown in Figure 3. In contrast, the joints of the groups with H/D=0.4 and H/D=0.75 had relatively large hole diameters but small laminate thicknesses. The combination of a large-diameter pin and a small-thickness composite resulted in a relatively uniform pin-hole contact through the laminate thickness.

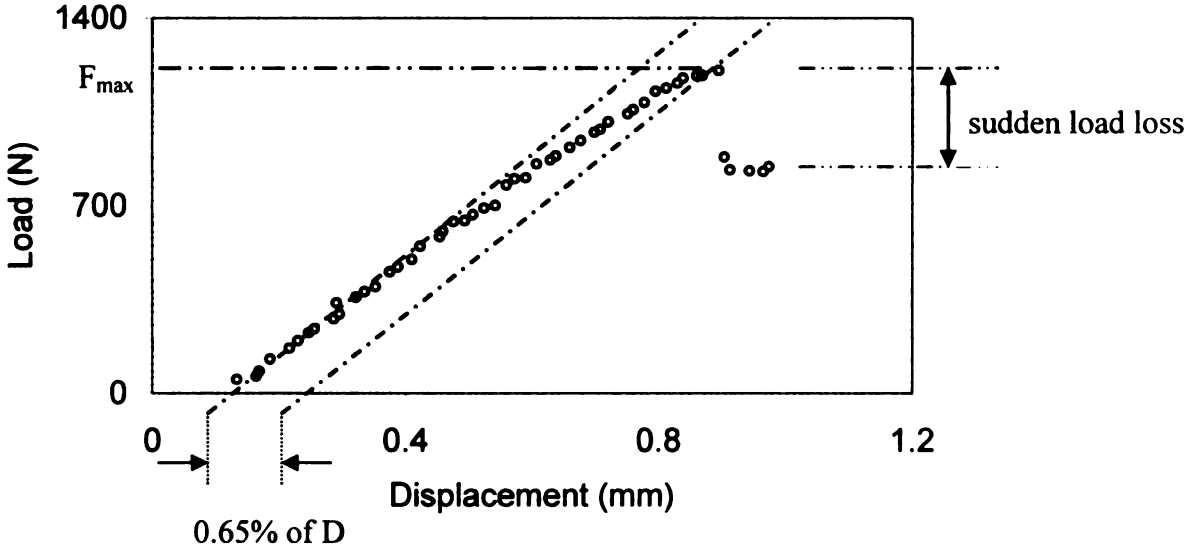

(a) brittle type (H8D2.77)

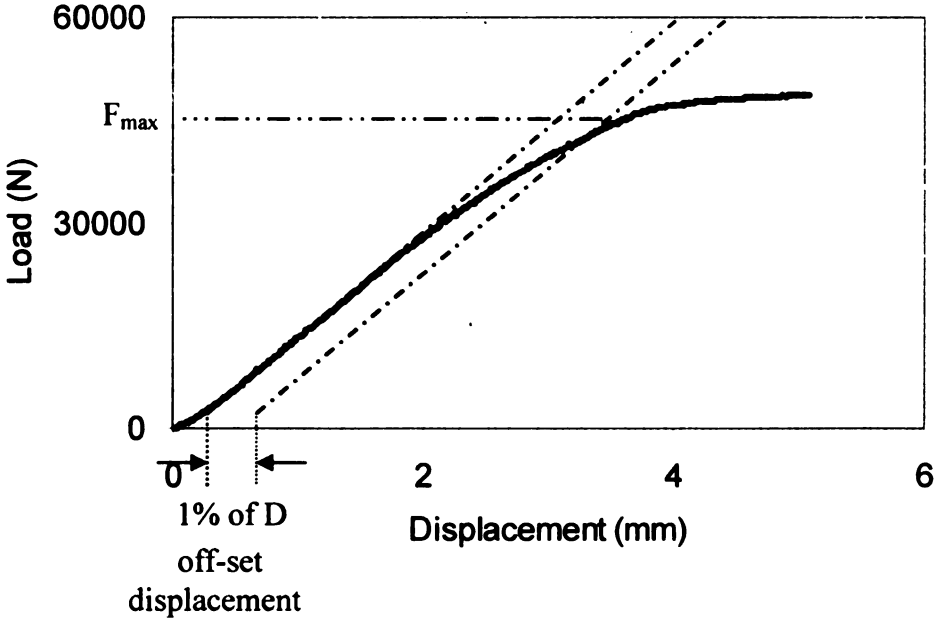

(b) ductile type (H80D12.7)

Figure 2 – Load-displacement curves, glass-fabric/phenolic composite joints

Table 2 – Types of load-displacement curves, maximum loads, and offset displacement percentage of all joints based on W-1 pins.

	T.[1]	Max.[2]	Off.[3]	T.[1]	Max.[2]	Off.[3]	T.[1]	Max.[2]	Off.[3]	T.[1]	Max.[2]	Off.[3]
	H8D2.77			H24D3.96								
	B	1.30	1.7	D	5.23	1.0						
	B	1.21	1.0	D	5.12	1.0						
	B	1.22	1.8	D	4.94	1.0						
	B	1.15	2.6	D	4.76	1.0						
	B	1.20	2.8	D	4.62	1.0						
	B	1.24	0.65	D	4.57	1.0						
Avg.(sd)[4]	1.22(0.05)			4.87(0.27)								
Average[5]	0.2248			0.2060								
	H8D5.16			H24D7.54			H40D6.35					
	B	2.00	1.16	B	11.11	0.45	D	14.00	1.0			
	B	2.01	0.76	B	11.39	0.37	D	12.13	1.0			
	B	2.12	0.67	B	12.05	0.40	D	12.62	1.0			
	B	2.17	0.61	B	12.22	0.49						
	B	2.13	0.53	B	11.37	0.90						
	B	2.01	0.38	B	11.48	0.93						
Avg.(sd)[4]	2.06(0.08)			11.60(0.43)			12.92(0.97)					
Average[5]	0.2034			0.2578			0.2165					
				H24D15.1			H40D12.7			H80D12.7		
				B	17.10	0.46	B	26.72	0.78	D	43.39	1.0
				B	15.61	0.59	B	24.01	1.8	D	30.50	1.0
				B	16.90	0.64	B	25.85	0.71	D	37.09	1.0
Avg.(sd)[4]				16.54(0.81)			25.44(1.38)			36.99(6.45)		
Average[5]				0.1836			0.2131			0.1428		
							H40D25.4					
							B	37.99	0.15			
							B	41.91	0.42			
							B	42.63	0.44			
Avg.(sd)[4]							40.84(2.50)					
Average[5]							0.1711					

[1] Type of load-displacement curve; B for brittle and D for ductile

[2] Maximum load (Unit: kN)

[3] Offset displacement percentage (with respect to hole diameter)

[4] Average maximum load (standard deviation) with a unit of kN

[5] Average bearing strength (Unit: GPa)

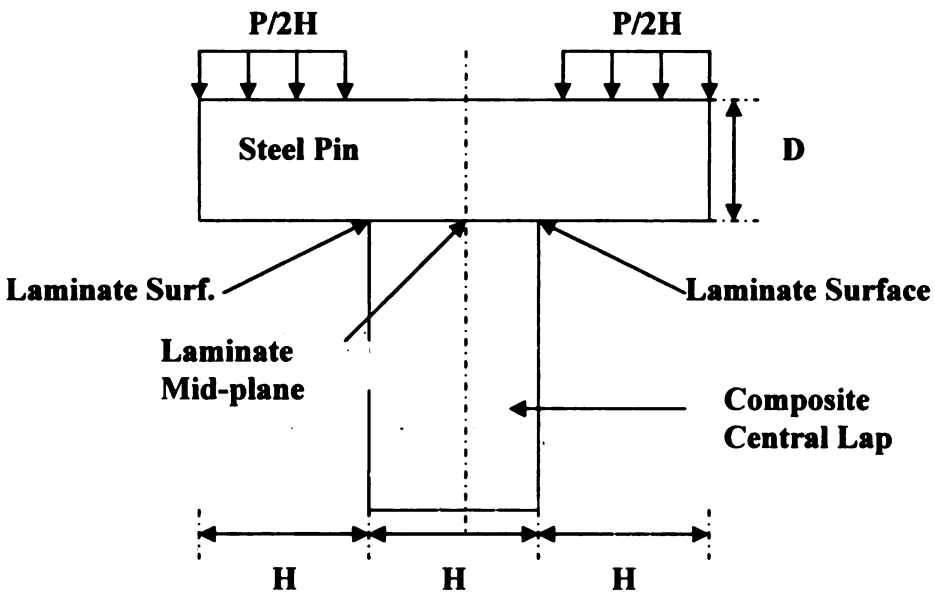

Figure 3 – Details of the shaded zone in Figure 1.

The correlation between the type of load-displacement curve and the geometric ratio H/D could be established by the following analysis. Figure 3 shows the core section of a double-lap-single-pin joint, which is the shaded zone given in Figure 1. Based on a strength-of-materials analysis, the maximum bending stress in the steel pin can be identified as

$$\sigma_{bending} = \frac{My}{I} = \frac{\frac{3PH}{8} \cdot \frac{D}{2}}{\frac{1 \cdot D^3}{12}} = \frac{9}{4}\frac{PH}{D^2}$$

Similarly, the averaged bearing stress in the composite central lap can be identified as

$$\sigma_{bearing} = \frac{P}{A} = \frac{P}{H \cdot 1} = \frac{p}{H}$$

Again, unit depth was used in the two-dimensional analysis. The ratio between the bending stress and the bearing stress can be found as

$$\frac{\sigma_{bending}}{\sigma_{bearing}} = \frac{9}{4}\left(\frac{H}{D}\right)^2$$

Thus, the type of load-displacement curve of a composite joint is dependent on the geometric ratio H/D of the joint. The failure of a composite joint with a large H/D ratio would be dominated by pin bending and have a ductile-type load-displacement curve. However, the failure of a composite joint with a small H/D ratio would be dominated by bearing failure of composite laminate and have a brittle-type load-displacement curve.

B. Damage Modes

To further understand the effect of the H/D ratio on the joint damage, some composite joints unloaded shortly beyond the occurrence of bearing failure were examined microscopically. All joint damage was identified to be fiber buckling. Both surface and

cross-sectional damage patterns were examined. In the surface investigation, the damage pattern below the holes was of primary concern. In the cross-sectional investigation, the damage pattern at the central cross-sections of composite laminate, shown in Figure 1, was of primary interest.

Except for those joints made of 8-ply laminates, two kinky bands could be clearly identified from the central cross-sections of the joints having brittle-type load-displacement curves. Each kink band ran from the laminate mid-plane to the laminate surfaces with an angle of 45° from the laminate mid-plane. The kink bands were formed by buckled fibers in every layer. Figure 4(a) shows the two kinky bands outlined by dotted lines in an H40D12.7 joint. The ends of the kink bands on the laminate surface at various cross-sections cumulatively formed an arch-shaped benchmark at a distance from the hole edge approximately equal to half the laminate thickness. Figure 4(b) shows the arch-shaped benchmark on the surface of an H24D7.54 joint.

Although the joints made of 8-ply laminates also had brittle-type load-displacement curves and fiber buckling damage, they did not have kink bands. The fibers buckled outward, namely outward buckling, as shown in Figure 4(c) with enhanced lines for an H8D5.16 joint. It was believed that the lesser constraint in the thickness direction due to the smaller laminate thickness was responsible for the outward buckling, instead of kink bands. A similar view has also been presented in a study concerning the compressive strength of composites by Zhang and Robert [64]. As a result of the outward buckling, there was no arch-shaped benchmark on the laminate surfaces.

The composite joints with ductile-type load-displacement curves had relatively complex damage patterns. Due to the large thicknesses, the damage patterns in these

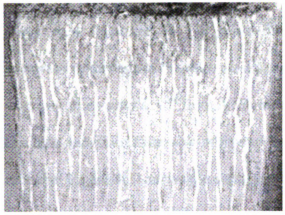

(a) central cross-section of H40D12.7

(b) surface of H24D7.54

(c) central cross-section of H8D5.16

(d) central cross-section of H80D12.7

(e) edge of 24-ply specimen

Figure 4 – Microscopic damage patterns of glass-fabric/phenolic composite laminates in joint/compression loading.

joints were expected to be non-uniform through the laminate thicknesses. The compressive damage in the plies close to laminate surfaces had kink bands although they were not necessarily at 45° from the laminate mid-plane. The damage in the plies close to laminate mid-planes was also attributed to kink bands but the kink bands were relatively irregular. Figure 4(d) shows the damage pattern of an H80D12.7 joint at the central cross-section. The associated surface damage pattern of the thick composite joint also had an arch-shaped benchmark. The non-uniform damage pattern through the laminate thickness revealed the non-uniform stress distribution through the laminate thickness, probably due to the non-uniform pin-hole contact in the joints with large H/D ratios. The pin-hole contact was apparently tighter in the plies close to the laminate surfaces than in the plies close to the laminate mid-plane. A tight contact resulted in a high compressive stress and 45° kink bands. A loose contact, however, resulted in a low compressive stress and non-45° fiber kinks.

C. Maximum Loads and Bearing Strengths

The composite joints investigated in the study all failed due to bearing damage. The joints with brittle-type curves had clear maximum loads. However, the joints with ductile-type curves had no clear maximum loads. The determination of the maximum loads for the joints with the ductile-type curves then required extra care. Since most of the joints with brittle-type curves reached their maximum loads at offset displacement levels around or less than 1% of the corresponding hole diameters, see Figure 2(a), a 1% hole diameter was chosen as the "yielding displacement" for determining the maximum loads of the joints exhibiting ductile-type curves. Once the maximum load of a joint was determined, it was normalized by the bearing area DH to give the average bearing

strength, i.e., P_{max}/DH. Both the maximum loads and bearing strengths of all composite joints are shown in Table 2.

2. 4 Various Effects

A. Effect Due to Stiffness of Outer-laps

In the present study, the outer laps of joints were made of steel, resulting in composite-steel dissimilar-material assemblies. Results from the present study were shown in Figure 5 along with those from the previous study [28], based on composite-composite similar-material assemblies, for comparison. The results of the dissimilar-material assemblies were represented by open symbols while those of the similar-material assemblies were represented by closed symbols. Although the geometric elements of the dissimilar-material assemblies and the similar-material assemblies are not exactly the same, they are very close. For example, the open circles are for H24D7.54 with steel outer laps while the solid circles are for H24D6.35 with composite outer laps. According to Figure 5, the bearing strengths of all the dissimilar-material assemblies are consistently higher than those of similar-material assemblies. For example, the difference between H24D7.54 and H24D6.35 is about 45%. This is more than what might be expected to be caused by the geometrical difference.

The difference in bearing strength between the two types of assemblies was believed to be due to the different contact conditions in the two types. Since the steel was more rigid than the glass-fabric/phenolic composite, the pin bending in the steel outer laps was smaller than in the composite outer laps. For example, H24D7.54 experienced an average of 0.59% offset displacement at failure while H24D6.35 experienced an average of 0.98%. Consequently, the pin-hole contact through the thickness of the composite central

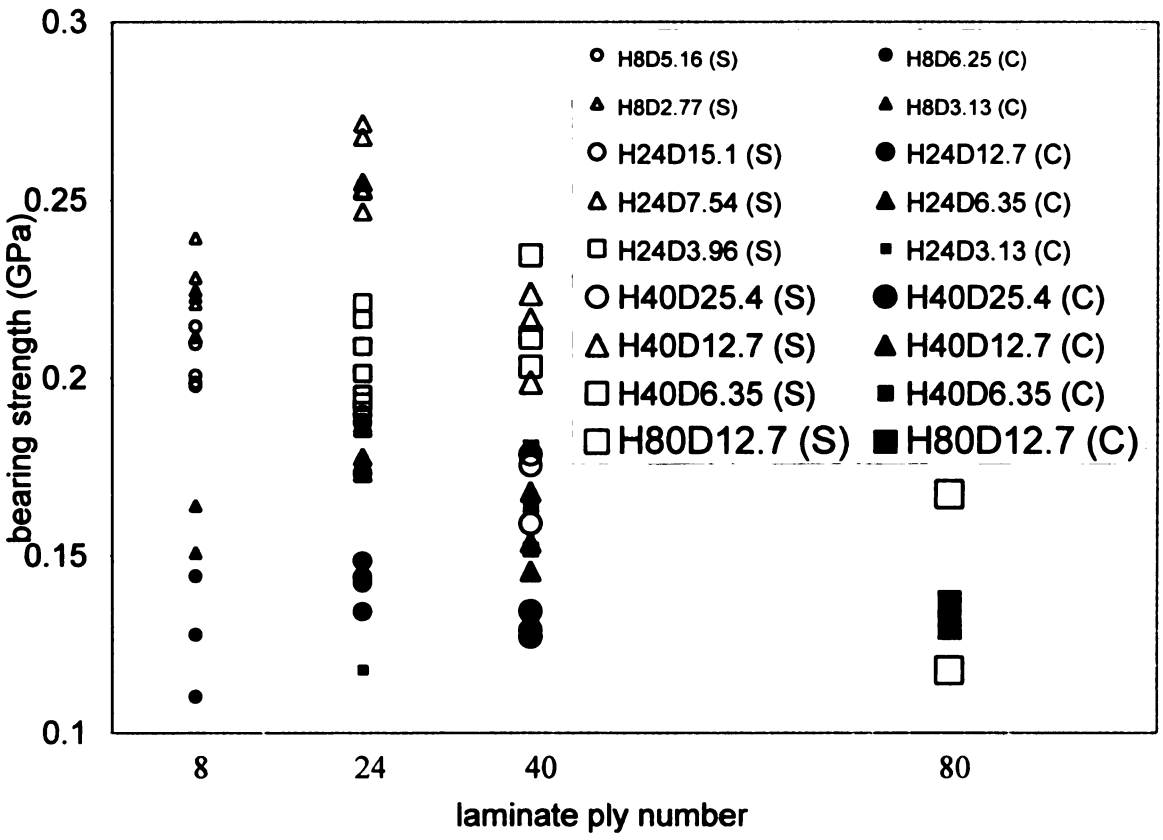

Figure 5 – Comparisons of bearing strengths between composite-composite assemblies and steel-composite assemblies (S for steel and C for composite central laps)

laps was more uniform in the steel-composite assemblies than in the composite-composite assemblies. A more uniform contact could avoid premature high stress concentrations at laminate surfaces and result in higher maximum loads, and subsequently higher bearing strengths, of composite joints.

B. Effects due to Pin Hardness

As mentioned earlier, the load-displacement curves of the joint groups with H/D=0.4 and H/D=0.75 were all of brittle type while those of H/D=1.5 were all of ductile type. When comparing the bearing strengths of composite joints in the different groups, a similar type of force-displacement curve, i.e. brittle-type, was preferred. Some efforts were made to change the type of load-displacement curves from ductile to brittle by using pins with higher hardnesses. Table 3 shows the results based on W-1, O-1 and M-2 pins for the joints having the smallest size in each group, i.e. H8D2.77, H8D5.16 and H24D3.96. As could be seen from Table 3, the change in bearing strength is not significant for the joints already having brittle-type curves, i.e. H8D2.77 and H8D5.16. However, there are noticeable changes in maximum loads for H24D3.96 joints. The average bearing strength increased by 22.6% when the M-2 pins were used to replace W-1 and O-1 pins. It was also found that M-2 pins could not change the type of load-displacement curves for joints made of 40-ply and 80-ply laminates.

Table 3 - Types of load-displacement curves, maximum loads, and offset displacement percentage of some joints based on various pins

	H8D2.77			H8D5.16			H24D3.96		
	Type[1]	Max. Load (kN)	Offset[2] (%)	Type[1]	Max. Load (kN)	Offset[2] (%)	Type[1]	Max. Load (kN)	Offset[2] (%)
W-1	B	1.30	1.7	B	2.00	1.2	D	5.23	1.0
pin	B	1.21	1.0	B	2.01	0.8	D	5.12	1.0
	B	1.22	1.8	B	2.12	0.7	D	4.94	1.0
	B	1.15	3.2	B	2.17	0.6	D	4.76	1.0
	B	1.20	2.2	B	2.13	0.5	D	4.62	1.0
	B	1.24	0.7	B	2.01	0.4	D	4.57	1.0
Avg.(sd)[3]		1.22(0.05)			2.06(0.08)			4.87(0.27)	
Average[4]		0.2248			0.2034			0.2060	
O-1	B	1.27	2.8	B	2.07	0.6	D	5.03	1.0
Pin	B	1.19	3.1	B	2.16	0.4	D	4.98	1.0
	B	1.19	1.0	B	2.03	0.5	D	4.82	1.0
	B	1.25	0.7	B	2.08	0.6	D	4.75	1.0
	B	1.18	1.4	B	2.08	0.4			
Avg.(sd)[3]		1.21(0.04)			2.09(0.05)			4.90(0.13)	
Average[4]		0.2236			0.2062			0.2072	
M-2	B	1.28	0.9	B	2.06	0.5	D	6.14	1.0
Pin	B	1.26	1.1	B	2.18	0.7	D	5.86	1.0
	B	1.30	2.0	B	2.03	0.5	D	6.02	1.0
	B	1.16	1.4	B	2.15	0.6			
	B	1.17	2.4	B	2.17	0.6			
Avg.(sd)[3]		1.23(0.06)			2.12(0.07)			6.01(0.14)	
Average[4]		0.2271			0.2092			0.2541	

[1] Type of load-displacement curve; B for brittle and D for ductile
[2]Offset displacement percentage (with respect to hole diameter)
[3]Average maximum load (standard deviation) with a unit of kN
[4]Average bearing strength (Unit: GPa)

The advantage of using high-hardness pins over low-hardness pins was essentially due to higher yielding stresses of the harder pins. The higher yielding stresses were associated with higher elastic limits, which reduced the pin bending to some extent. Accordingly, the non-uniform pin-hole contact through the laminate thickness could be improved and thus a higher bearing strength achieved.

C. Effect Due to Compressive Strength

No matter whether outward buckling or kink bands occurred, the damage of the pin joints investigated in the study was due to compressive fiber buckling. Compressive strength is, therefore, an important parameter in the damage analysis. To further understand the damage processes in compression, some compressive tests have been performed. Specimens based on 24-ply and 40-ply laminates were prepared and their dimensions were three-dimensionally scaled. In performing the compressive tests, anti-buckling devices similar to those suggested by ASTM D695 standard were built and used in the tests.

The damage mode of the specimens subjected to compressive loading was different from those subjected to pin loading. Instead of fiber buckling, such as outward buckling and kink bands, two shearing fractures were found in each damaged specimen, shown by the enhanced lines in Figure 4(e). In addition, rather than initiating from the mid-plane as the kink bands did in the pin joining cases, each shearing fracture started from a contact location close to a laminate surface. The shearing fractures extended with an average angle of about 20° to the laminate mid-plane of a 24-ply specimen and eventually merged together. The average angle of the shearing fractures in the 40-ply specimens was around 30°.

The differences in damage mode and strength were significant between the cases subjected to pin joining and compressive loading. The average compressive strength of the 24-ply specimens was 0.136 GPa while that of 40-ply specimens was 0.118 GPa. Apparently, the compressive strengths were much lower than the bearing strengths given in Table 2. A similar result has also been reported by Collings [65]. Besides the difference of loading mode, another possible interpretation of the discrepancy could be based on the outward bulging of the central laps due to compression. The outward bulging beneath the pin-hole contact could create some sort of interlocking and clamping between the central laps and the outer laps. In fact, it has been shown by some researchers [56, 66, 67] that a small clamping force could improve joining strength by 30-100%. A large bolting force has even been found to produce a 300% increase in joint strength [68].

2. 5 Size Effects

All the pin joints investigated in the study were based on three-dimensional scaling. The three cases of the group with H/D=0.4 were scaled from 8 to 24 and to 40, i.e. a 1:3:5 scaling ratio. The three cases of the group with H/D=0.75 had an identical scaling ratio as the cases of the group with H/D=0.4. The three cases of the group with H/D=1.5 were scaled from 24 to 40 and to 80, i.e. a 1:1.67:3.33 scaling ratio.

The bearing strengths of the group with H/D=0.4 decreased by 9.2 and 15.4% as the size increased by three times and five times, respectively, resulting in a monotonic decrease of bearing strength with the increase of joint size. The bearing strengths of the groups with H/D=0.75 increased by 14.7% then decreased by 5.6% as the size increased to three times and five times. Similarly, the bearing strengths of the group with H/D=1.5

increased by 5.1% then decreased by 30.7% as the size increased to 1.67 times and then 3.33 times. Both the groups with H/D=1.5 and H/D=1.5 had non-monotonic changes of bearing strength with the increase of joint size. The non-monotonic changes in the groups with H/D=0.75 and 1.5 were believed to be associated with higher thickness effects than the monotonic decrease in the group with H/D=0.4. That is, the higher the H/D ratio, the higher the thickness effect. The bearing strengths of all the joints are listed in Table 2. They are also shown graphically in Figure 6.

The changes of bearing strength with the increase of joint size were not monotonic in the groups with H/D=0.75 and 1.5. They actually increased then decreased. Thus, the three-dimensional size effect in the pin joints was not Weibull type, which states that the strength of materials always decreases with the increase of size. This discrepancy might be associated with the difference of damage mode. As mentioned earlier, the smallest cases (made of 8-ply laminates) of the groups with H/D=0.4 and H/D=0.75 had a damage mode of outward buckling while the medium and the largest cases (made of 24-ply and 40-ply laminates) had a damage mode of kink bands. Both the differences in bearing strength (monotonic and non-monotonic) and damage mode (outward buckling versus kink bands) implied that both material properties and geometrical parameters should be considered in the three-dimensional size effect.

In an effort to understand why the three-dimensional size effect was not Weibull-type, the three-dimensional scaling was divided into in-plane scaling and thickness scaling. The in-plane scaling and the thickness scaling were investigated individually and the results are presented in Figure 7 and Figure 8 (based on Liu et al. [28]), respectively. In the studies of in-plane size effect and thickness size effect, only joints with brittle-type

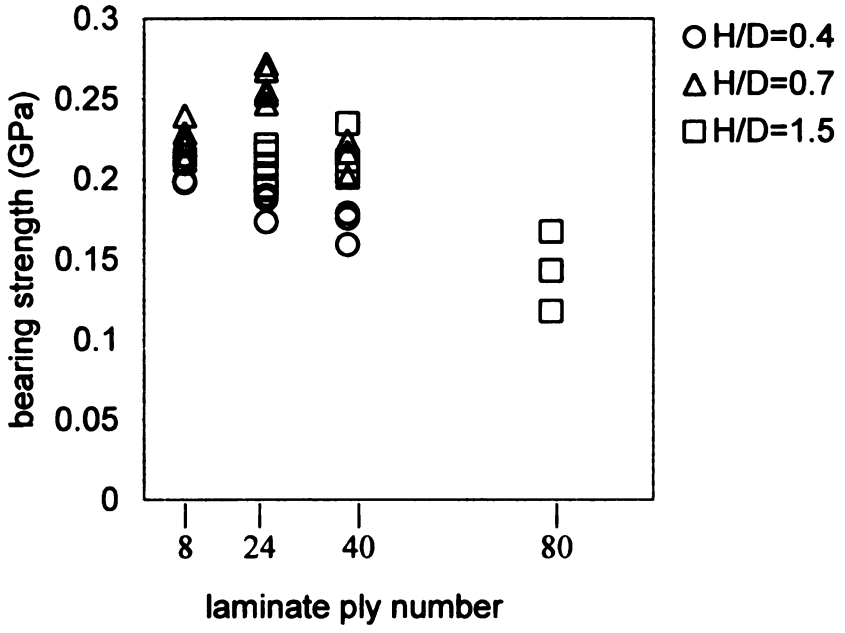

Figure 6 – Bearing strengths due to three-dimensional scaling.

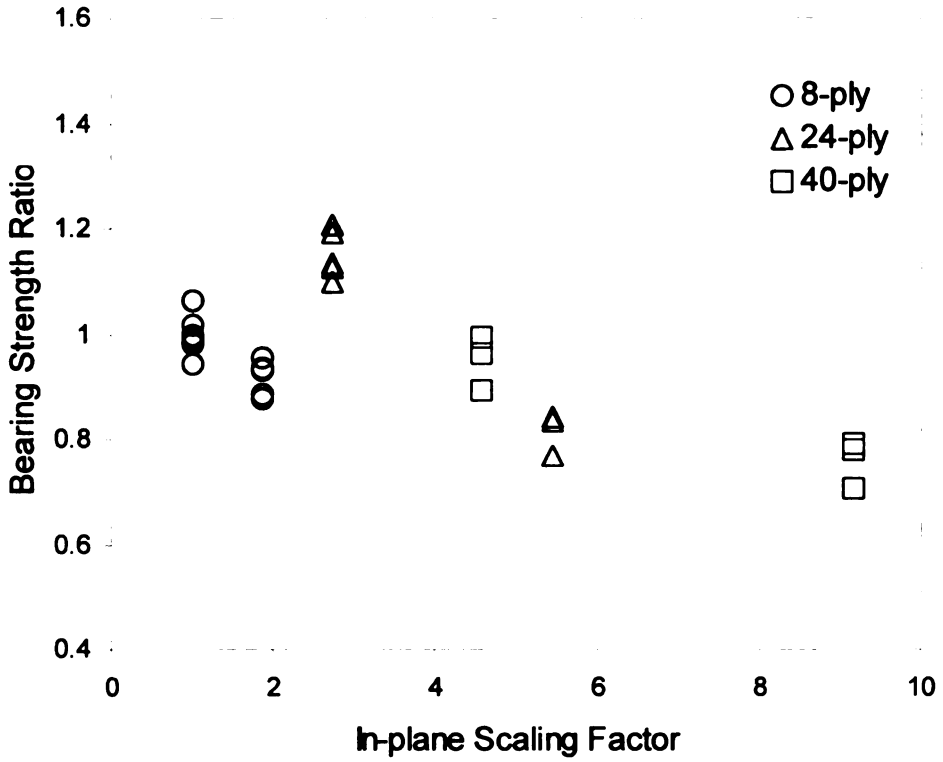

Figure 7 – Bearing strength ratios (bearing strengths normalized by that of H8D2.77) due to in-plane scaling.

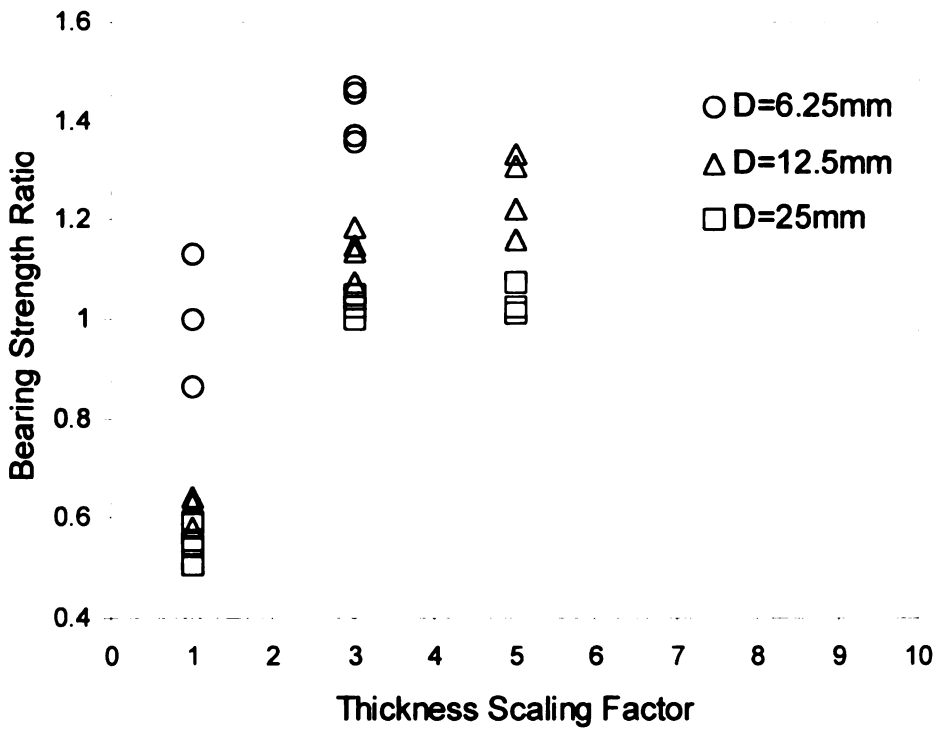

Figure 8 – Bearing strength ratios (bearing strengths normalized by that of H8D6.25) due to thickness scaling.

damage were included since brittle-type damage was better defined than ductile-type damage.

In the study of the in-plane size effect, the bearing strength of the H8D2.77 joint was used to normalize the strengths of all joints. As shown in Figure 7, there were three groups, designated as 8-ply, 24-ply and 40-ply. In each group, the thickness is kept constant while the in-plane dimensions are scaled. It could be seen from Figure 7 that the bearing strength in each group decreases as the in-plane scale increases. Similar results for the in-plane size effect have also been reported in the literature for specimens without crack [18] and with cracks [16]. Apparently, the Weibull theory [17, 18] is capable of interpreting the in-plane size effect because the Weibull theory is essentially based on the argument that larger specimens have larger defects and hence have lower strengths. In addition, it is interesting to point out that the theory of Bazant et al. [16] is also capable of interpreting the in-plane size effect because the Bazant theory, based on fracture mechanics, predicts that the reduction rate of strength with the increase of size is approximately equal to 1/2 for large isotropic, brittle specimens.

In the study of the thickness size effect, the bearing strength of H8D6.25 was used to normalize the strengths of all the joints. There were three groups in the study [28], designated as D6.25, D12.5 and D25. In each group, the in-plane dimensions were kept constant while the thickness was scaled. It could be seen from Figure 8 that the bearing strengths in each group increase as the thickness scale increases. A similar result based on the thickness study has also been reported by Wang et al [19]. The interpretation of the change in bearing strength due to the thickness scaling was more complicated than that due to in-plane scaling. In addition to the negative influence based on the Weibull

theory for specimens subjected to pin loading (also true for specimens subjected to compressive loading reported in the section "Effect Due to Compressive Strength"), there was apparently a positive contribution due to the thickness scaling. The damage of pin joints was essentially due to fiber buckling, and hence the increase of thickness constraint was expected to greatly increase the buckling resistance of fibers. However, as the thickness increased, the risk to pin bending also increased. Thus, the increase of bearing strength due to increase in thickness was a combined result of the positive contribution from the increase in buckling resistance and the negative influences from the Weibull-type size effect and pin bending.

Based on the negative influence from the in-plane scaling and the resultant positive contribution from the thickness scaling, the three-dimensional size effect of the pin joints could be postulated as follows. The resultant three-dimensional size effect in pin joints was not monotonic because of a negative influence and a positive contribution. The three-dimensional size effect was not Weibull-type, which is essentially based on material defects. Although the non-monotonic effect was based on pin joints with brittle-type damage, i.e. H/D=0.4 and 0.7, this conclusion could be extended to the pin joints with ductile-type load-displacement curves, i.e. H/D=1.5.

Geometrical scaling, such as in-plane scaling and thickness scaling, are directly responsible for size effects. They can also affect the material properties of composite laminates to some extent. For example, the size of material defects such as microcracks, voids, resin-rich pockets, etc., can be affected by the thickness scaling of composite laminates. Since composite laminates are constructed by plies, the properties of composite laminates are usually not constant through the laminate thickness because non-

uniform curing temperature histories are experienced in individual plies [24, 69] even if the plies have an identical fiber orientation. This phenomenon can become significant as composite thickness increases. Besides, the associated thermal residual stresses are also likely to increase as the thickness and hence the geometrical constraint in the thickness direction increases. Thus, as a material defect, the thermal residual stress due to composite curing may impose a size effect in the composite laminates.

2. 6 Conclusions

Based on experimental results and discussions, the following conclusions can be drawn from the investigations of pin joints:

1. The steel-composite joints had higher bearing strengths than the composite-composite joints because the higher constraint imposed by the stiffer steel outer laps, which renders a more uniform pin-hole contact.

2. Steel pins with higher hardnesses seem to give more uniform contacts through the laminate thicknesses, resulting in higher bearing strengths.

3. Composite laminates subjected to compressive loading had different damage modes and lower strengths than those subjected to pin loading.

4. For in-plane scaling, the bearing strength decreases as the size increases. For thickness scaling, the bearing strength increases as the size increases. For three-dimensional scaling, the bearing strengths change non-monotonically as the size increases for the groups with H/D=0.75 and 1.5.

Chapter 3

Scaling Effects and Thickness Constraints in Composite Joints

3. 1 Introduction

Joining is a secondary process in structure manufacturing. In manufacturing conventional metallic structures, small components are fabricated individually and then assembled to form large sections. Although complex polymer composite structures can be molded in single pieces to simplify manufacturing processes and to reduce assembly cost, they cannot be completely exempted from the joining process. The joining process is especially needed when polymer composite components are to be assembled with components made of dissimilar materials such as metals.

Both mechanical fastening and adhesive bonding are commonly used in structure assembling. As structure components to be assembled become thicker, both the diameter and length of mechanical fasteners should be increased proportionally. Similarly, the bonding areas in the plane and through the thickness [11] of the structure components should be increased in adhesive bonding. The increase in the diameter and length of mechanical fasteners and the increase in the bonding areas of adhesive bonding, however, are not purely geometrical scaling issues. Material properties should also be considered as the size increase.

The studies of scaling for composite structures can be divided into in-plane scaling, thickness scaling and three-dimensional scaling. In studying in-plane scaling, thin composite laminates with notches [16] and without notches [18] were investigated. The strengths of composite laminates were found to decrease monotonically with the increase of in-plane dimensions. In a two-dimensional study on mechanical fastening, Wang et al.

[19] reported that the bearing strength had a first-decrease-then-increase change as the in-plane dimensions increased.

Thickness also plays an important role in composite size scaling [1, 3-6]. In fact, there is a special concern in scaling the thickness of composite laminates. Being different from simply increasing or decreasing the thickness in scaling the thickness of conventional metals, there exists at least two different ways in scaling the thickness of composite laminates, so-called sub-laminate scaling and ply-thickness scaling. The thickness scaling is actually more complicated than in-plane dimension scaling since both material properties and geometrical parameters are involved in the thickness scaling. More specifically, the non-uniform material properties induced by thickness scaling and the non-uniform stresses through laminate thickness caused by fastener bending due to large thickness [25-27] render the study very complicated. In a previous study [28], the thickness effect in composite pin joints was found to be dependent on the ratio of laminate thickness H to hole diameter D, i.e. H/D. Joint configurations with ratios of H/D around one were found to have more adequate performance than those with ratios of H/D greater than one.

Combining the in-plane dimension scaling and the thickness scaling, the three-dimensional size scaling needs to be understood before designers could predict the performance of large composite assemblies based on the properties of small models, especially when thick composite laminates are of primary concern. The objective of this study is to investigate the effects of three-dimensional size scaling on the performance of composite mechanical fasteners.

3. 2 Experimental Methods

A. Joint Configurations

Composite laminates made from glass/epoxy prepreg tapes were investigated in the study. Cross-ply laminates were of interest. They were made with alternate 0^{o} and 90^{o} plies and their stacking sequences can be expressed by $[0/90/0/90\ldots]_n$ where n is the total number of plies. Three composite laminates having 9 plies (n=9), 17 plies (n=17) and 34 plies (n=34) were prepared. Their thicknesses were 3.30mm, 6.48mm and 12.95mm, respectively.

The double-lap-single-pin joint shown in Figure 1 was used as the experimental model. The glass/epoxy composite laminates were used as central laps of joints while steel plates were used as outer laps, resulting in steel-composite dissimilar-material joints. The steel outer plates had thicknesses half those of composite central laps, warranting that the damage of joints was dominated by the damage of composite central laps. For mechanical fastening, steel pins designated as M-2 according to AISI classification system were used. The hardness of the steel pins was in the range of 63-65 based on the Rockwell C Hardness standards.

Figure 1 shows the geometrical elements of composite joints. These elements include the joint width W, the hole diameter D, the laminate thickness H, the distance between the hole center and the joint end E, and the distance between the hole center and the gripping end L, also called joint length. The associated geometrical ratios W/D, E/D, H/D and L/W are also important parameters in studying mechanical fastening. In order to have bearing damage, at least initially, instead of net-section damage or shear-out damage, W and E were chosen to be four times the hole diameter, resulting in W/D=4 and E/D=4.

For identification purposes, each composite joint was assigned with a notation of HXDY, where H and D were laminate thickness and hole diameter, respectively, while X and Y were the ply number of the composite laminate and the hole diameter in millimeter (mm), respectively.

In investigating three-dimensional size effects, three composite joints were prepared based on three-dimensional scaling. Since the composite laminates used in the study had a thickness scaling ratio of 1:1.97:3.92, i.e. 3.30mm:6.48mm:12.95mm, the closest integer ratio of 1:2:4 was used for scaling all other dimensions D, W and E. Since H/D was an important parameter in the thickness study and H/D=1 was found to be the critical value for composite joints to have load-displacement relations with distinct maximum loads in Chapter 2, the hole diameter was chosen to be as close to the laminate thickness as possible. Based on the availability of drill bits and M2 pins, hole diameters of 3.18mm (1/8"), 6.35mm (1/4") and 12.7mm (0.5") were used in the study, resulting in H9D3.18, H17D6.35 and H34D12.7 joints. Details of the geometrical elements and geometrical ratios of the three composite joints are given in Table 4.

B. Joint Lengths

As mentioned earlier, the distance between the hole center and the gripping end, i.e. the joint length, was designated as L. Although this distance is the key parameter associated with Saint Venant's end effect, it was not exercised in the three-dimensional scaling due to the limited sizes of the composite laminates available and the length confinement of the testing machine used. In fact, the joint length L for the joints H9D3.18, H17D6.35 and H34D12.7 were 241.3mm, 228.6mm and 203.2mm, respectively, resulting in L/W=19, 9 and 4, respectively. In order to verify that the joint

Table 4 – Geometrical elements and ratios of glass/epoxy central laps.

Unit: mm	H9D3.18	H17D6.35	H34D12.7
H	3.30	6.48	12.95
D	3.18	6.35	12.70
W	12.70	25.40	50.80
E	12.70	25.40	50.80
L	241.3	228.6	203.2
H/D	1.04	1.02	1.02
W/D	4.00	4.00	4.00
E/D	4.00	4.00	4.00
L/W	19.00	9.00	4.00

H: thickness
D: hole diameter
W: width
E: distance from hole center to specimen end
L: distance between hole center and gripping end

length had insignificant effect on joint performance when L/W had a minimum value of 4, H9D3.18 joints with L/W=9, 4, and 1.5 were investigated. These specimens were designated as H9D3.18-L/W9, H9D3.18-L/W4, and H9D3.18-L/W1.5.

C. Pin-Hole Clearances

Pin-hole clearance has significant effects on joint performance [54]. Studies concerning the effects of bolt-hole clearance on bearing stress distributions are also available in the literature, e.g. References [70-73]. These studies were focused more on joint performance prior to final failure than on ultimate joint strength. Pierron et al. [74] investigated the effects of pin-hole clearance on bearing strength. The clearances used in their study were higher than 0.1mm. It was concluded from their study that minimum clearance was optimum for joint designs.

In the present study, pins having the same sizes as hole diameters, i.e. so-called snug fitting between pins and holes, were initially used in H9D3.18, H17D6.35 and H34D12.7 joints. In order to assess the effects of pin-hole clearance on joint performance, additional efforts were exercised for H9D3.18 joints. Besides the standard pins that had a diameter of 3.18mm, pins with diameters of 3.15mm, 3.11mm and 3.09mm, i.e. with pin-hole clearances of 0.03, 0.07 and 0.09mm, respectively, were also prepared. The composite joints having large pin-hole clearances were designated as H9D3.18-pc0.03, H9D3.18-pc0.07 and H9D3.18-pc0.09.

D. Loading Rates

The epoxy matrix of the composite material used in the study was of a viscoelastic material. The behavior of the composite material was thus expected to be sensitive to loading rate [75-77]. Studies concerning the effects of loading rate on composite

performance were reviewed by Sierakowski [78]. Ger et al. [79] and Li et al. [80] even studied the performance of composite joints under various impacting rates. Although the investigation of composite joints was usually performed at a quasi-static loading rate, there was no consensus on the definition of quasi-static loading rate in the material testing community. In an experimental report on mechanical fasteners [81], the loading rate was set to be 1mm/min. In a second experimental report on pin-joint structures [19], the relative speed between the loading heads was 1.27mm/min. In a third report [80], the loading rate of static tensile tests was set to be 0.5mm/min.

In engineering practice, the quasi-static loading rates could vary from a very small level up to 5mm/min as recommended by ASTM D638 for tensile testing of composite laminates. In the present study, the effects of loading rates on joint performance were of interest. The loading rate of 1.27mm/min was considered to be the basic loading rate because it was commonly used in material testing. This loading rate was applied to all three types of composite joints. In order to investigate the effects of loading rate on joint performance, loading rates of 0.16mm/min (1/8 of 1.27mm/min), 0.64mm/min (1/2 of 1.27mm/min) and 5.08mm/min (four times 1.27mm/min) were also applied to H9D3.18 joints. They were designated as H9D3.18-lr0.16, H9D3.18-lr0.64 and H9D3.18-lr5.08.

3. 3 Joint Properties

A. Load-Displacement Relations

Load-displacement relations bore important information concerning properties of joints. Beyond the initial linear ranges, all load-displacement curves seemed to exhibit two different types of profiles that could be categorized as ductile type and brittle type. Figure 9 gives an example for each type. The ductile-type curve shown in Figure 9(a) was

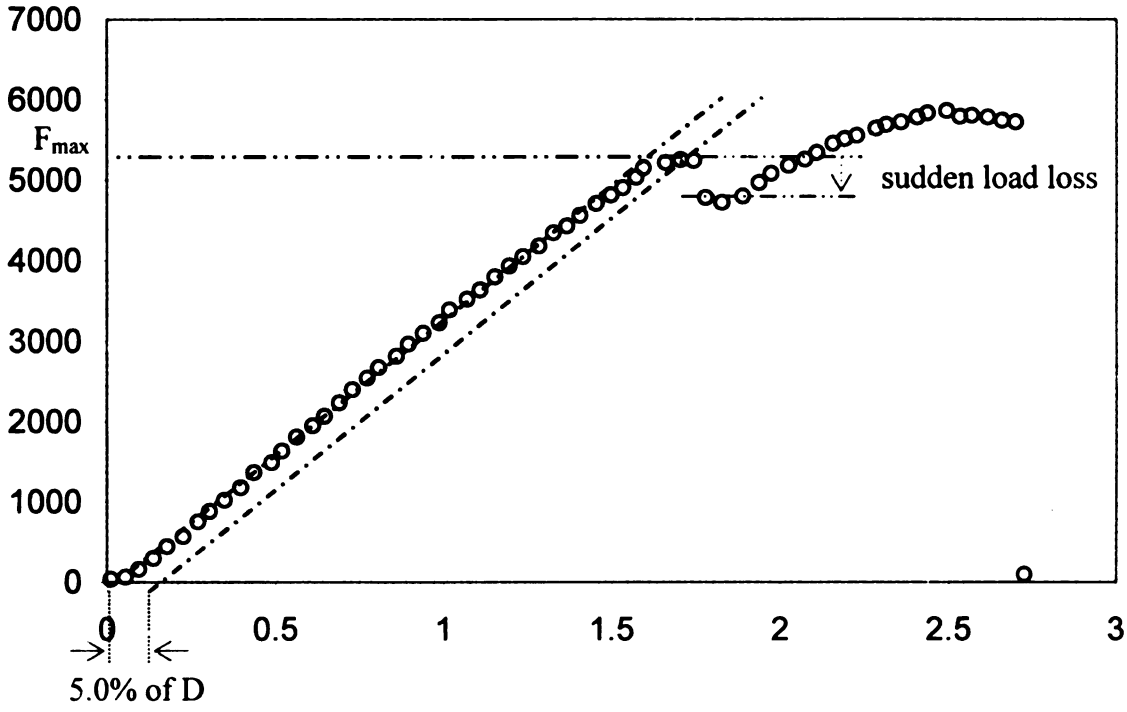

(a)

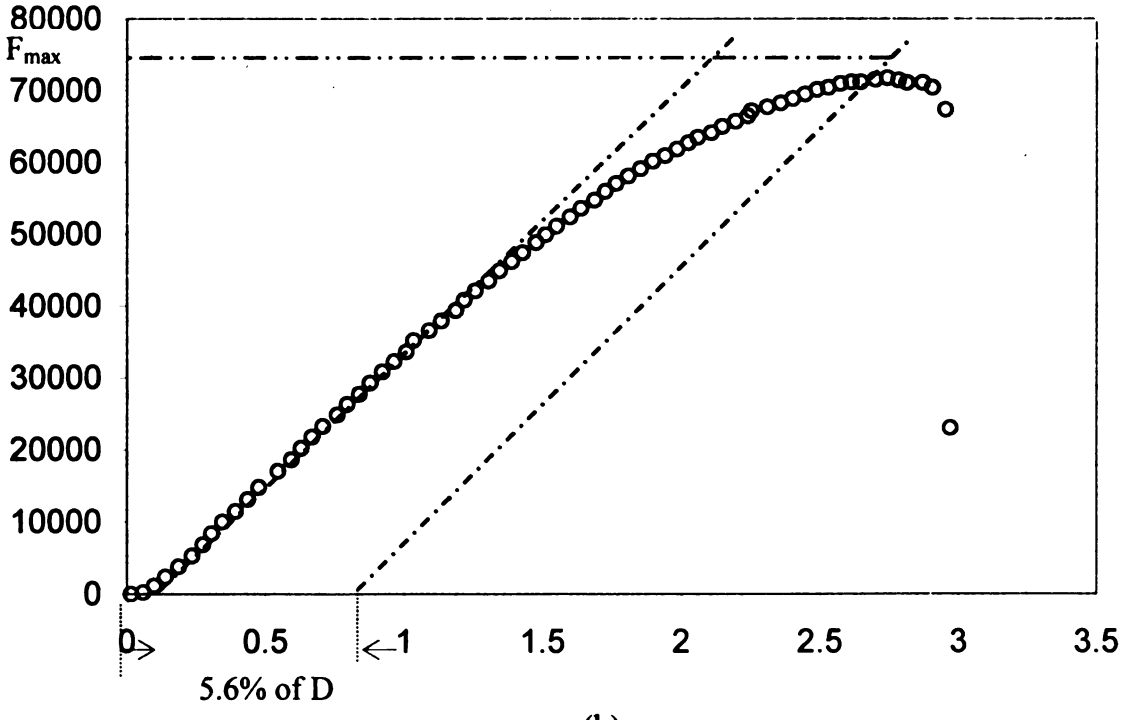

(b)

Figure 9 – Load-displacement (N-mm) curves, glass/epoxy composite joints. (a) ductile type (H9D3.18) and (b) brittle type (H34D12.7).

obtained from an H9D3.18 joint. It featured a small but noticeable loss in load right after a local maximum load. This loss in load was found to be associated with bearing damage. The value of load usually recovered as loading process continued before another load loss occurred. This second load loss, however, was drastic and non-recoverable and was found to be associated with the net-section damage. The brittle-type curve shown in Figure 9(b) was based on an H34D12.7 joint. It showed a continuously smooth relation until a catastrophic drop of load, which was found to be associated with net-section damage, occurred.

B. Maximum Loads and Joint Strengths

Based on Figures 9(a) and 9(b), the strengths of composite joints may be defined by the maximum loads. An "offset of displacement" associated with the maximum load was also presented for further evaluations. The "offset of displacement" was defined as the distance between the initial linear segment of a load-displacement curve and a line passing through the maximum load and parallel to the linear segment. A term named "percentage of offset of displacement" was further defined as the percentage of the ratio of the "offset of displacement" to the hole diameter. The presentation of the "percentage of offset of displacement" was aimed at justifications of maximum loads. According to Table 5, the percentages of offsets of displacement of all joints ranged from 4 to 7%. The identifications of maximum loads for joints with different types of load-displacement relations, i.e. the ductile type and the brittle type, were thus justified. Once the maximum loads of joints were identified, they were divided by corresponding bearing-contact areas, i.e. DH, to determine the bearing strengths. The maximum loads, percentages of offset of

Table 5 – Types of load-displacement curves, maximum loads and percentage of offset of displacement of various glass/epoxy joints.

	T.[1]	Max.[2]	Off.[3]	T.[1]	Max.[2]	Off.[3]	T.[1]	Max.[2]	Off.[3]	T.[1]	Max.[2]	Off.[3]
	H9D3.18			H9D3.18-L/W9			H9D3.18-L/W4			H9D3.18-L/W1.5		
	D	5.18	5.0	D	5.29	6.2	D	5.37	5.2	D	4.48	6.2
	D	5.89	6.8	D	4.78	6.8	D	5.50	6.0	D	5.08	6.2
	D	4.54	5.8	D	5.46	5.2	D	5.78	7.0	D	5.83	6.8
	D	5.27	7.7	D	5.50	5.9	D	5.34	4.5	D	5.30	5.3
	D	4.86	5.4	D	5.87	6.7	D	4.97	6.6	D	5.67	5.5
	D	5.70	6.2							D	5.01	4.8
	D	5.47	7.0							D	5.69	5.7
	D	5.49	6.7							D	5.41	6.3
	D	5.52	6.2							D	4.67	5.1
	D	5.32	7.1							D	5.00	6.5
	D	5.85	5.2							D	5.85	8.2
										D	5.23	6.8
Avg.(sd)[4]	5.37(0.41)			5.38(0.40)			5.39(0.29)			5.25(0.44)		
Avg. Strength[5]	512.66			513.30			515.32			501.09		
	H9D3.18-pc0.03			H9D3.18-pc0.05			H9D3.18-pc0.09			H9D3.18-lr0.16		
	D	4.32	4.4	D	4.52	4.2	D	4.23	5.2	D	4.89	3.1
	D	5.27	5.0	D	5.24	4.2	D	4.80	4.3	D	4.89	5.8
	D	5.60	5.9	D	4.64	4.8	D	4.76	4.4	D	5.00	5.1
	D	5.25	6.2	D	4.84	5.1	D	4.65	5.0	D	4.47	4.5
	D	4.85	5.7	D	4.91	4.2	D	4.38	3.8	D	4.26	4.9
										D	4.77	4.7
										D	5.01	5.3
Avg.(sd)[4]	5.06(0.49)			4.83(0.28)			4.56(0.25)			4.76(0.29)		
Avg. Strength[5]	482.46			461.06			435.36			453.80		
	H9D3.18-lr0.64			H9D3.18-lr5.18			H17D6.35			H34D12.7		
	D	4.95	5.7	D	5.48	4.5	D	17.66	5.3	B	70.07	4.8
	D	4.58	6.4	D	5.85	4.3	D	18.19	3.8	B	71.80	5.6
	D	5.15	6.4	D	5.19	4.6	D	16.91	4.4	B	71.90	5.3
	D	5.07	6.4	D	6.15	5.7	D	17.15	5.0			
	D	5.08	5.2	D	4.97	5.1	D	19.19	6.0			
	D	5.33	6.3	D	5.21	4.9						
	D	5.01	5.2	D	6.21	5.2						
	D	4.68	5.2	D	5.66	6.0						
	D	5.24	4.4	D	5.60	4.9						
	D	5.38	5.2	D	5.30	4.5						
				D	5.62	5.0						
				D	6.04	6.4						
Avg.(sd)[4]	5.05(0.26)			5.61(0.40)			17.82(0.91)			71.25(1.03)		
Avg. Strength[5]	481.62			535.15			433.14			431.85		

[1] Type of load-deformation curve: B for brittle and D for ductile;
[2] Maximum load (Unit: kN); [3] Percentage of offset of displacement at maximum load;
[4] Average load (standard deviation) with a unit of kN; [5] Average strength (Unit: MPa).

displacement and average joint strengths of all composite joints were given in Table 5 along with the types of load-displacement curves.

C. Macroscopic and Microscopic Damage Modes

Because it was less catastrophic than net-section damage and shear-out damage, bearing damage was preferred in the failure of mechanical fasteners. Accordingly, W/D=4 and E/D=4 were imposed to all joints in order to have bearing damage, at least initially. However, not all composite joints investigated in the study started failure with initial bearing damage. Composite joints of H9D3.18 and H17D6.35 had initial bearing damage prior to ultimate net-section failure. However, the dominant damage mode of H34D12.7 joints was the direct catastrophic net-section failure. In an effort to further understand the process of damage, microscopic damage modes in the neighborhood of bearing-contact zones were also examined.

Figure 10 shows the microscopic damage of an H17D6.35 joint. As shown in Figure 10(a), there are matrix cracks along the net-section lines and delamination underneath the bearing-contact zone. On the cross-section along the laminate centerline, zig-zag kinks can be found in the 0^{o} plies as shown Figure 10(b). The fiber kinks were the results of fiber buckling due to the high compressive stress around the contact-bearing zone. The microscopic damage of H9D3.18 was similar to that of H17D6.35. However, the microscopic damage around the bearing zones of H34D12.7 joints was relatively insignificant; only very few fiber kinks were found in the 0^{o}-plies close to the laminate surfaces. It seemed a correlation between macroscopic damage and microscopic damage could be established.

(a) Front View

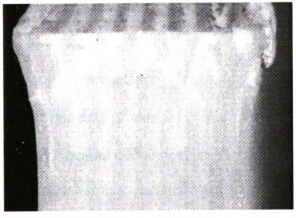

(b) Cross-sectional view

Figure 10 – Microscopic damage in an H17D6.35 glass/epoxy joint.

3. 4 Experimental Results

A. Effect of Joint Lengths

From experiments, the average joint strengths of H9D3.18-L/W9, H9D3.18-L/W4 and H9D3.18-L/W1.5 were 513.3, 515.3 and 501.1MPa, respectively. Both H9D3.18-L/W9 and H9D3.18-L/W4 had average strengths very close to 512.7MPa of the H9D3.18 joints, whose L/W=19. In other words, the joint strengths seemed to remain constant as the ratio of L/W surpassed 4. Accordingly, the uses of different ratios of L/W for H9D3.18, H17D6.35 and H34D12.7, i.e. 19, 9 and 4, respectively, were considered to have no significant effect on the joint performance.

B. Three-dimensional Size Effects

In the experimental study, the joint length L between the hole center and the gripping end were chosen to be at least four times the joint width W. The joint width W and the distance between the hole center and the joint end E were chosen to be exactly four times the hole diameter D. The hole diameter D was chosen to be close to the laminate thickness H. Hence, the laminate thickness H can be considered as the most fundamental scaling parameter. Based on the laminate thickness of the three composite joints H9D3.18, H17D6.35 and H34D12.7, the thickness scaling 3.30mm:6.48mm:12.95mm, i.e. 1:1.96:3.92 or approximately 1:2:4, was used in the study of three-dimensional scaling.

As shown in Table 5, the average joint strengths of H9D3.18, H17D6.35 and H34D12.7 were 512.7, 433.1 and 431.9MPa, respectively. The joint strength decreased by 15.5% and 15.8% as the joint size doubled and quadrupled, respectively, from H9D3.18. The average joint strength had a monotonic decrease as the joint size increased.

This result seemed to be comparable with that based on Weibull's theory. The experimental results and Weibull analysis were also presented in Figure 11 for comparisons. In fact, the feasibility of using Weibull's theory in three-dimensional size scaling is an important issue in mechanical fastening designs.

Weibull theory was a statistical analysis. It stated that the larger the size of a material, the larger the size of defect in the material, and hence the lower the strength of the material. In order to examine the feasibility of using Weibull's theory in three-dimensional size scaling of composite joints, the two-parameter Weibull theory [82] was used in strength analysis. According to the two-parameter Weibull theory, the probability of failure P_f can be expressed as

$$P_f = \exp^{-\frac{v}{v_o}(\frac{\sigma}{\sigma_o})^m} \tag{1}$$

where m is the Weibull modulus and σ_o is the normalizing strength. They are the two parameters of the Weibull's theory. Besides, v is the volume and v_o is the normalizing volume. The above equation can be rewritten as follows by taking nature log twice on both side of the equation, i.e.

$$\ln(\ln(\frac{1}{P_f})) = \ln\frac{v}{v_o} + m\ln\sigma - m\ln\sigma_o \tag{2}$$

The first term on the right-hand side of the equation vanishes when the concerned specimens have constant dimensions. The reduced equation is usually assumed to be of a straight line. The Weibull modulus and the normalizing strength can then be found from curve fitting such as the least-squares method.

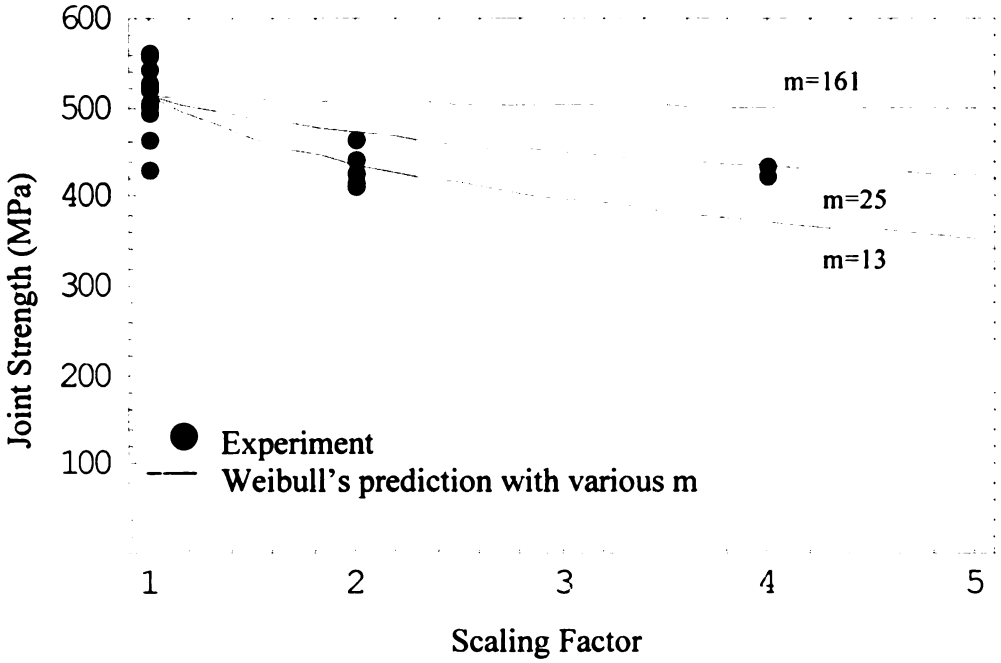

Figure 11-- Glass/Epoxy joint strengths of different sizes and analysis based on Weibull theory.

The Weibull moduli for the three joints H9D3.18, H17D6.35 and H34D12.7 were found to be 13, 25, and 161, respectively. The higher the Weibull modulus, the smaller the variation of strength. However, it was noted that the small joint H9D3.18, having the largest number of testing specimens, seemed to have much larger variation than the larger joints H17D6.35 and H34D12.7 which had smaller number of testing specimens (five for H17D6.35 and three for H34D12.7). If the lowest modulus, i.e. m=13, along with the volume v_1 and the strength of H9D3.18, i.e. σ_1=512.7MPa, were used for three-dimensional scaling analysis, the scaled strengths of H17D6.35 and H34D12.7 could be calculated from the following equation

$$\left(\frac{\sigma}{\sigma_1}\right)^m = \frac{v_1}{v} \tag{3}$$

where σ and v are the corresponding strength and volume of H17D6.35 and H34D12.7 joints. As can be seen in Figure 4, the Weibull's theory, based on m=13, seems to predict a clearer size effect than that obtained from limited tests. Weibull's predictions based on m=25 and m=161 are also presented in Figure 4 for comparison. It seems Weibull's theory agrees with the experimental results up to some extent.

C. Effect of Pin-Hole Clearances

From experiments, the average joint strengths of H9/D3.18-pc0.03, H9/D3.18-pc0.07 and H9/D3.18-pc0.09 were found to be 482.5, 461.1 and 435.4MPa, respectively. These strengths were lower than the average strength of H9D3.18, i.e. 512.7MPa, which had a snug fit between the pin and the hole. Based on these experimental data, it was clear that the joint strength decreased as the pin-hole clearance increased. An explanation for this

result could be based on the change of contact area between the pin and the hole. As the pin-hole clearance increased, the contact surface between them decreased, as verified by Eriksson [70] based on a numerical simulation. The decrease in contact area increased the contact-bearing stress and subsequently decreased the joint strength.

D. Effect of Loading Rates

The average joint strength of H9D3.18 under a loading rate of 1.27mm/min was 512.7MPa. The average joint strengths of H9D3.18 at different loading rates, e.g. 0.16mm/min (H9D3.18-lr0.16), 0.64mm/min (H9D3.18-lr0.64) and 5.08mm/min (H9D3.18-lr5.08), were 453.8, 481.6 and 535.2MPa, respectively. When compared all four cases together, it was found that the joint strength increased with the increase of loading rate. This result was consistent with some reports in the literature. For instance, Waas et al. [76] had found that the dynamic strength of a glass/epoxy composite could be as high as 1.7 times the static values. The result that the higher the loading rate, the higher the joint strength could also be applied to joint stiffness.

3. 5 Assembled and Laminated Composites

A. Assembling Techniques

Thick composite laminates have many applications in heavy-duty structures such as armored vehicles. However, their costs are high and their properties are not uniform due to uneven curing cycles, especially in the thickness direction [24, 69]. Assembling thin composite laminates together to form thick composite structures was found to be feasible in reducing cost and achieving property uniformity. Techniques such as adhesive bonding, riveting and clamping were presented in previous studies on assembled composites [83, 84]. It was found that the impact resistance of assembled composites was

very comparable with that of laminated counterparts. The present study investigated mechanical fasteners in both assembled and laminated composites. The comparisons of joining strengths and damage processes were of primary interests.

In studying assembled composites, two 9-ply laminates were bonded together with a room-curing epoxy to form an assembled composite. Because the total thickness of the assembled composite was close to that of H17D6.35 laminated composite, for comparison purpose, a resembling 6.35mm-diameter hole was prepared in the assembled composite for mechanical fastening. For identification purpose, the assembled composite was designated as H9x2D6.35-B where B stands for bonded. If the two 9-ply laminates were simply put together and contacted each other without any form of bonding, a notation of H9x2D6.35-C (C for contacted) was used for the assembled composite. The geometric elements and ratios of the mechanical fasteners made of the assembled composites were similar to those of the laminated counterpart, i.e. H17D6.35, so were the experimental parameters.

In a similar investigation, four 9-ply laminates were bonded together to form an assembled composite. Since it had a total thickness close to that of the 34-ply laminates, i.e. H34D12.7, a hole of 12.7mm in diameter was prepared in the assembled composite for mechanical fastening. A notation of H9x4D12.7-B was used to identify the assembled composite. Similarly, a notation of H17x2D12.7-B was used for an assembled composite bonding two 17-ply laminates together.

B. Normalized Strengths

Table 6 gives experimental results of the joints. Besides the averaged strengths, normalized strengths are also presented in the table. The normalized strengths were

Table 6 – Comparison between laminated and assembled glass/epoxy joints.

	T.[1]	Max.[2]	Off.[3]	Mode[4]	T.[1]	Max.[2]	Off.[3]	Mode[4]	T.[1]	Max.[2]	Off.[3]	Mode[4]
Pinned	H9x4D12.7-B				H17x2D12.7-B				H34D12.7			
	D	73.99	4.2	BR	D	67.19	5.7	BR	B	70.07	4.8	NS
	D	76.32	3.8	BR	D	64.91	5.2	BR	B	71.80	5.6	NS
	D	73.53	5.8	BR	D	69.67	7.0	BR	B	71.90	5.3	NS
Avg.(sd)[5]	74.61(1.50)				67.25(2.38)				71.25(1.03)			
Avg. Strength[6]	421.31				410.09				431.85			
Norm. Strength[7]	21.06				22.79				25.48			
Pinned	H9x2D6.35-C				H9x2D6.35-B				H17D6.35			
	D	19.20	2.7	BR	D	20.38	5.1	BR	D	17.66	5.3	BR
	D	19.32	3.6	BR	D	19.90	6.6	BR	D	18.19	3.8	BR
	D	18.76	4.1	BR	D	19.55	4.3	BR	D	16.91	4.4	BR
					D	19.82	5.4	BR	D	17.15	5.0	BR
									D	19.19	6.0	BR
Avg.(sd)[5]	19.10(0.29)				19.91(0.35)				17.82(0.91)			
Avg. Strength[6]	435.16				453.80				433.14			
Norm. Strength[7]	43.52				45.38				48.13			
Bolted	H9x2D6.35-C				H9x2D6.35-B				H17D6.35			
	B	20.65	7.4	NS	B	21.23	5.4	NS	B	19.87	5.8	NS
	B	20.46	7.0	NS	B	21.45	7.4	NS	B	19.35	3.8	NS
	B	20.44	6.9	NS	B	21.35	7.1	NS	B	20.31	4.2	NS
Avg.(sd)[5]	20.52(0.12)				21.34(0.11)				19.84(0.48)			
Avg. Strength[6]	467.56				486.44				482.34			
Norm. Strength[7]	46.76				48.64				53.59			

[1] Type of load-deformation curve: B for brittle and D for ductile

[2] Maximum load (Unit: kN)

[3] Percentage of offset of displacement at maximum load

[4] Failure mode at maximum load: BR for bearing and NS for net-section

[5] Average maximum load (standard deviation) with a unit of kN

[6] Average maximum load per contact area --- DH (Unit: MPa)

[7] Average strength normalized by the number of 0^{o} plies (Unit: MPa)

obtained from dividing averaged joint strengths by corresponding numbers of layers that had fibers oriented in the loading directions. The normalized strengths were presented due to the fact that the laminated composites and the assembled counterparts did not have the same numbers of total layers, nor did they had the same numbers of layers with fibers oriented in the loading directions, i.e. 0^{o}-direction in the present study. For example, the laminated composite H34D12.7 had a total number of 34 plies; and only 17 out of the 34 plies were in the 0^{o}-direction. The assembled counterpart H9x4D12.7-B had a total number of 36 plies; and only 20 out of the 36 plies were in the 0^{o}-direction.

Experimental results of the joints based on assembled composites and laminated counterparts are given in Table 6. The normalized strengths of the two assembled composites H9x4D12.7-B and H17x2D12.7-B were 10% lower than that of the laminated counterpart, i.e. H34D12.7. However, the normalized strengths of the bonded composite H9x2D6.35-B and unbonded composite H9x2D6.35-C were about the same as that of the laminated counterpart, i.e. H17D6.35. It seemed the assembled composites could resemble the laminated composites up to some extent, at least, as far as mechanical fastening was concerned.

C. Ultimate Failure

Besides the joint strength, another important experimental result was associated with the damage process. All specimens investigated in the study seemed to fail with initial bearing damage except H34D12.7, which experienced direct catastrophic net-section damage. The interpretation of this phenomenon is stated as follows. Being compared with H9x2D6.35-B, H9x2D6.35-C and H17D6.35, H34D12.7 was more constrained in the thickness direction due to its larger thickness. Being compared with H9x4D12.7-B and

H17x2D12.7-B, H34D12.7 was more constrained in the thickness direction due to its better bonding through the laminate thickness. Accordingly, the constraint in the thickness direction played a key role in the damage process. A composite with more constraint in the thickness direction had higher resistance to fiber buckling and delamination, resulting in direct catastrophic net-section damage. In contrast, a composite with less constraint in the thickness direction was more prone to fiber buckling and delamination. For example, the H17D6.35 joint shown in Figure 10(a) resulted in initial bearing damage prior to final net-section damage.

Although their geometrical elements and ratios were about the same, H9x4D12.7-B, H17x2D12.7-B and H34D12.7 joints had different damage processes. The former two types had initial bearing damage prior to finial net-section damage while the latter one had direct catastrophic net-section damage. Initial bearing damage was an important damage mode in composite fasteners as shown in Chapter 2, at least in thin composites. The primary mechanism of the bearing damage was fiber buckling and delamination. They rendered composite joints more ductile. Shown in Figure 12 are the load-displacement curves of the aforementioned three joints. Although H34D12.7 had the highest normalized strength, it had the lowest displacement to failure. The total energy absorbed by H34D12.7 due to damage formation, which was equal to the area under the load-displacement curve, was also smaller than those absorbed by the assembled counterparts, i.e. H9x4D12.7-B and H17x2D12.7-B. In fact, it was easier to have delamination on the assembled interfaces than on the laminated interface because the adhesive bonding strength on the assembly interfaces was lower than the matrix bonding

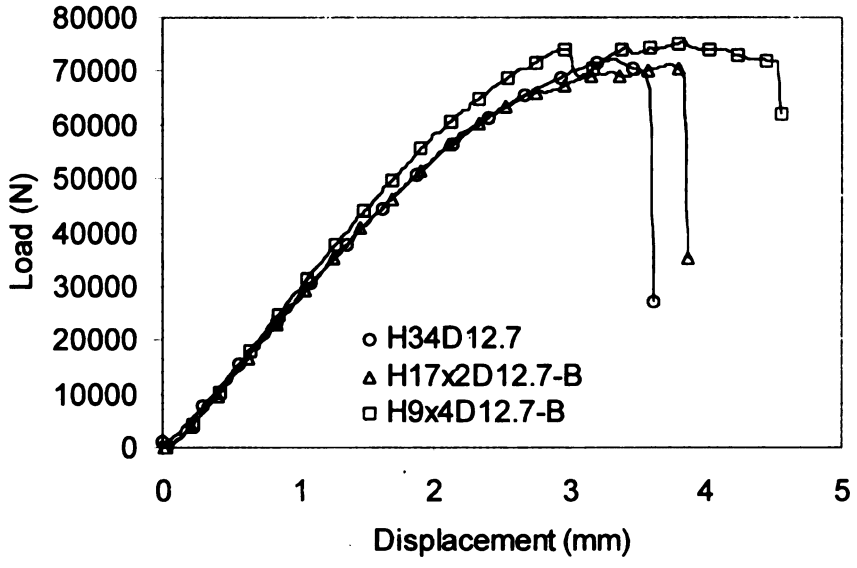

Figure 12 – Load-displacement curves of assembled (bonded) and laminated glass/epoxy joints.

strength on the laminated interfaces. Once delaminated, the disassembled thin laminates were prone to fiber buckling and delamintion, i.e. the bearing damage. In contrast, the laminated counterpart H34D12.7 was not vulnerable to delamination, except those interfaces very close to the laminate surfaces. As a result, the bearing damage was insignificant in H34D12.7 joints. They failed by direct catastrophic net-section damage.

3. 6 Difference Between Pinned and Bolted Joints

A. Constraints in Thickness Direction

As mentioned earlier, the constraint in the thickness direction played a key role in the damage process of composite fasteners. The higher the constraint in the thickness direction, the higher the resistance of composite to fiber buckling and delamination. Hence, a composite joint with high constraint in the thickness direction, such as H34D12.7, would result in direct catastrophic net-section damage, i.e. a relatively brittle-type failure. However, a composite joint with low constraint in the thickness direction, such as H9x4D12.7-B, would result in initial bearing damage prior to final failure, i.e. a relatively ductile-type failure. Another way to verify the shift of failure mode from a ductile type to a brittle type as the constraint in the thickness direction increased was to compare pinned joints with bolted counterparts since the latter had additional constraints, i.e. clamping forces, in the thickness directions.

B. Bolted Joints

Although pinned joints were commonly used in research studies, bolted joints were more practical in structure assembly. In fact, the clamping force used in bolted joints seemed to enhance the joining strength [85, 86]. Matthews et al. [87] had shown that a

pinned joint had the lowest strength, a fully bolted joint had the highest strength, while a riveted joint had a strength between the two extremes.

In comparing the pinned and the bolted joints, H17D6.35, H9x2D6.35-B and H9x2D6.35-C joints were used. The clamping force for the bolted joints was 20 Nm. The experimental results were given in Table 6. The normalized strengths of the bolted joints were slightly higher than those of the pinned counterparts. This result was consistent with that obtained from the comparisons among H9x4D12.7-B, H17x2D12.7-B and H34D12.7 cases.

There was also a shift in damage mode due to the increase of constraint in the thickness direction. For pinned joints, i.e. H9x2D6.35-B and H9x2D6.35-C, the damage modes showed initial bearing damage prior to final net-section damage; for bolted counterparts, however, direct catastrophic net-section damage dominated. Since the only variation introduced was the clamping force in the thickness direction, this result further verified the important role of the through-the-thickness constraint in the behavior of joints. Apparently, the high constraint due to clamping force rendered the composite joints higher resistance to delamination. Accordingly, direct catastrophic net-section damage, instead of initial bearing damage followed by final net-section damage, took place in the bolted joints.

In summary, the constraint in the thickness direction played a key role in both joining strength and damage process. A composite with a higher constraint based on larger thickness, better bonding through the thickness or clamping force in the thickness direction could increase the joining strength slightly. However, the higher constraint in the thickness direction rendered the composite more brittle, i.e. smaller displacement to

failure and smaller energy absorption during failure process, and resulted in direct catastrophic net-section damage, instead of initial bearing damage followed by final net-section damage.

3. 7 Conclusions

1. The load-displacement curves of the mechanical fasteners investigated in the study can be categorized as ductile type and brittle type. Both H9D3.18 and H17D6.35 joints had ductile-type load-displacement curves while H34D12.7 joints had brittle-type curves. The "percentage of offset of displacement" was presented to determine the maximum loads and the subsequent joint strengths.
2. There was a monotonic decrease in joint strength as the three-dimensional size increased. The reduction of joint strengths seemed to agree with the Weibull's theory up to some extent. Although the final failure of all joints was due to net-section damage, the joints with the ductile-type load-displacement curves experienced initial bearing damage prior to final net-section damage while the joints with the brittle-type load-displacement curves failed by direct catastrophic net-section damage.
3. The constraint in the thickness direction played a key role in the damage process of composite fasteners. In addition to large thickness, good bonding through the thickness and adequate clamping force from bolting also contributed to the constraint in the thickness direction.
4. High constraint in thickness direction prevented fibers from bucking and composites from delamination. Composite joints with high constraints in the thickness direction failed in direct catastrophic net-section damage while those

with low constraint in the thickness direction failed with initial bearing damage prior to final net-section damage.

5. Composite joints that failed with initial bearing damage had higher displacement to failure and higher energy absorption during failure process than those that failed with direct catastrophic net-section damage.

Chapter 4

Three-dimensional Finite Element Analysis of Composite Pin Joints

4. 1 Introduction

Composite materials are originally developed for use as aerospace structures. They are thus of thin plates. The in-plane behavior of composite plates has been the focus of composite research in the past few decades. As more composite materials are used for non-aerospace applications, there are more thick-section composites structures, e.g. submarine hull and armored vehicle bodies. The extension from thin composite plates to thick-section composites, however, is not a trivial practice. In fact, it requires careful modifications in many aspects of composite technologies, e.g. manufacturing, testing, analysis and design [1-7].

Taking composite joining as an example, both adhesive bonding and mechanical fastening are commonly used in joining composite plates. Adhesive bonding is in fact a two-dimensional joining technique as it takes effect only at the contact areas between the structural components being joined. Mechanical fastening, on the contrary, is a three-dimensional joining technique. Both diameters and lengths of mechanical fasteners should increase as the thickness of the structure components increase. Hence, adhesive bonding is more adequate for joining thin composite plates while mechanical fastening can be used for joining thick-section composites [11].

The three-dimensional nature of mechanical fastening in composite joining was experimentally recognized by some researchers [28, 88]. The significant effect of composite thickness on the efficiency of pin joint was reported [28], so was the key role of thickness constraints in the damage process as discussed in Chapter 3. The effects of thickness on composite pin joints were found to be associated with the ratio of composite

thickness (H) to hole diameter (D), i.e. H/D, as in literature [28] and Chapter 2. If H/D is smaller than 1.0, it refers to a composite joint consisting of relatively thin plates and a relatively large pin. On the contrary, if H/D is greater than 1.0, it refers to a composite joint is consisting of relatively thick sections and a relatively small pin. As the H/D ratio changes from smaller than 1.0 to greater than 1.0, both the type of the load-displacement curve and the strength of the composite joint change significantly due to the change of the contact condition between the composite and the pin

Many analytical studies concerning mechanical fastening were presented and most of them were based on two-dimensional assumptions. As mentioned by Oplinger [25], all two-dimensional studies ignored the details of stress distribution through the thickness of the fasteners. Nelson, Bunin and Hart-Smith [26] also presented important insights of the thickness effects on fastener bending. The importance of using three-dimensional techniques in studying mechanical fastening was also recognized by other researchers [27, 29-31]. Ireman [27] found that the bending of a bolt created a non-uniform contact stress distribution between the bolt and the hole. According to Chen, Lee and Yeh [30], the bolt elasticity had a tendency to change the stress distribution through the laminate thickness.

Besides the nonuniform contact through the length of the bolt, the nonuniform properties of composites through their thickness posed more challenges to the investigations of composite joints. Among the very few studies based on three-dimensional analysis, the interlaminar stresses between different layers were often not examined thoroughly. An investigation based on a three-dimensional spline variational technique was conducted by Iarve and Schaff [31] to analyze the interlaminar stresses in

a composite fastener. Shokrieh and Lessard [32] studied a pin-joint structure with radial displacement boundary conditions. Stress singularities were reported at the interface between layers with different ply orientations on the free edges. However, the contact stress and friction between the pin and the plate were not considered in their study.

Some studies, including References [33-36], were focused on predicting the strength of joint structures solely based on the stress distribution on the hole surface. Their studies belonged to the category of so-called one-parameter failure analysis in which the maximum stress, maximum strain or distortional energy on the hole surface was input into a failure criterion to assess the status of the joint structure. The one-parameter failure analysis was simple to use but did not account for the composite response near the hole. Hart-Smith [37] reported that the ultimate joint failure could be attributed to the damage near the hole, instead of right at the hole surface. The one-parameter failure analysis based on the large stress on the hole surface could underestimate the strength of the composite joints.

The idea of two-parameter failure analysis was similar to Whitney-Nuismer's work, which was focused on hole size effects in composite plates. A characteristic dimension [38], which was normally a certain distance away from the hole in the laminate plane, was required in a two-parameter failure theory. Two failure theories were proposed by them; one was the so-called point stress failure theory and the other was the average stress failure theory. The characteristic dimension was considered as a material property in early studies for two-parameter failure analysis. Later investigations [39, 40], however, proved that it was dependent upon laminate quality and type of load. Furthermore, it was concluded that the predicted failure loads were quite sensitive to the value of

characteristic dimension [39, 41] or the shape of characteristic curve [42]. Thus, the two-parameter failure theories were problem dependant and could not be used straightforward.

With the assumption that damage took place in the zones where a failure criterion was satisfied, some progressive damage models were proposed to simulate the damage initiation. Besides, with the use of elastic property degradation as a function of the degree of composite damage, the progressive damage models were further used to simulate the damage growth [43-47]. The predicted failure loads were in good agreement with experimental results for open holes subjected to compression and tension by Chang and Lessard [48] and by Chang, Liu and Chang [49], respectively. However, it seemed that the good experimental correlation could be partially attributed to the fact that the authors used the best fitted fiber failure interaction zone introduced by Tsai [50]. Furthermore, it was noted that the damage growth in the compression case [48] was sensitive to the finite element mesh and the authors adopted a specific mesh to obtain the known damage propagation for each composite lay-up. This manipulation disabled the generalization of the computational modeling for various lay-ups and geometries. For loaded holes [51], no improvement in accuracy was found in predicting the joint strengths with the use of a progressive damage model [42, 52].

Instead of accounting for the many microscopic damage modes in the failure analysis as Chang [44], Tan [53] modeled the stiffness degradation of composite laminate in a more global sense. No specific damage modes were considered in his failure analysis. Once damage took place, the degradation of a composite property was represented by the product of its initial value and a corresponding factor. The predicted strengths were in

close agreement with experimental results for several types of lay-up. However, it was found that the results were very sensitive to the degradation factors used.

Aiming at understanding more insights of the damage process of composite joints, this study was to analyze the stress distributions around the critical area of a composite joint and to investigate the suitability of existing failure criteria. Several stress-based failure criteria under the one-parameter failure theory were compared. A two-parameter failure theory was also included for discussions.

4. 2 Finite Element Modeling

A. Composite Materials and Mechanical Fasteners

As investigated in two previous chapters, a double-lap-single-pin joint, as shown in Figure 1, was of primary interest. The central lap was made of a glass/epoxy laminate with a stacking sequence of $[0/90/0/90...]_9$ while the outer laps were made of steel. Each ply of the composite laminate was considered as a transversely isotropic material. Details of the material properties are given in Table 7. A steel pin designated as M-2 according to AISI classification system was used to assemble the composite lap and steel laps together, resulting in a dissimilar-material joint.

In investigating a mechanical joint, some geometrical parameters are essentially important. Their definitions are shown in Figure 1. That is, the width of the joint W, the diameter of the hole D, the thickness of the laminate H, the distance between the center of the hole and the free end of the laminate E, and the distance between the center of the hole and the gripping end of the laminate L, also called the joint length. In this particular study, a model with H= 3.30mm, D= 3.18mm, W= E= 12.70mm and L =50.8mm was identified as a basic model, resulting in the following geometrical ratios: H/D= 1.04,

Table 7 – Material properties of glass/epoxy laminate (3M Aerospace Systems Lab).

	Notation	Value
Exx	Longitudinal moduli	39.3GPa
Eyy=Ezz	Transverse/Normal moduli	8.3GPa
Gxy=Gxz	x-y/x-z shear moduli	3.1GPa
Gyz	y-z shear moduli	2.9GPa
νxy=νzx	x-y/z-x Poisson's ratio	0.26
νyz	y-z Poisson's ratio	0.30
Strength data		
Xt	Longitudinal tensile	965MPa
Xc	Longitudinal compression	880MPa
Yt	Matrix tensile	31MPa
Yc	Matrix compression	118MPa
Sxy=Szx	x-y/z-x shear	72MPa
Syz	y-z shear	26MPa
Microscopic properties		
γ_y	Longitudinal shear yield strain	0.024 (1.4^0)
ϕ_0	Initial fiber misalignment	2^0

W/D= 4, E/D= 4 and L/W=4. For identification purpose, this model was named as H/D=1. Two other models, H/D= 0.5 and H/D= 2 were also investigated. The complete geometrical parameters and geometrical ratios of all three models are given in Table 8.

B. Finite Element Model

A coordinate system XYZ, as depicted in Figure 13, originated at the center of the hole and the mid-plane of the composite laminate was established. An angular coordinate θ measured from X axis was also established in the X-Y plane. The joint geometry and loading condition were symmetric with respect to the X-Y and X-Z planes. Hence, only one quarter of the joint model needed to be examined. The quarter composite lap is denoted by ACDEIFGH and symmetric boundary conditions are applied on both ACDE plane and ACGF plane. The nodes on CDHG plane were deprived of all degrees of translational freedom, simulating the fixed boundary conditions imposed by the grip fixture depicted in Figure 1. In addition, quarter the joining and loading pins and quarter the central loading plate as well as half one outer steel lap were included in the model. Figure 14 shows the model in the finite element analysis. With regard to loading, normal tensile forces were applied to the bottom plane of the central loading plate.

Key locations on composite plate around the hole were specifically denoted for studying the stress distributions and the damage process of the mechanical joints. As shown in Figure 15, B_0 (bearing) is located at Z= 0 and $\theta = 0^0$ while N_0 (net-section) at Z= 0 and $\theta = 90^0$. It is worth noting that both B_0 and N_0 are located in the mid-plane of the most inner 0^0-ply of the $[0/90/0/90\ldots]_9$ composite laminate, i.e. right at the mid-plane of the composite laminate. The Z/H ratios for both B_0 and N_0 are zero as the X-Y plane, i.e. the plane of Z= 0, coincides with the mid-plane of the composite laminate.

Table 8 – Geometrical elements and ratios of three simulation models.

	H/D=1	H/D=1/2	H/D=2
H (mm)	3.30	3.30	3.30
D (mm)	3.18	6.36	1.59
W (mm)	12.70	25.40	6.35
E (mm)	12.70	25.40	6.35
L (mm)	50.8	101.6	25.4
H/D	1.04	0.52	2.08
W/D	4.00	4.00	4.00
E/D	4.00	4.00	4.00
L/W	4.00	4.00	4.00

H: thickness
D: hole diameter
W: width
E: distance from hole center to specimen end
L: distance between hole center and gripping end

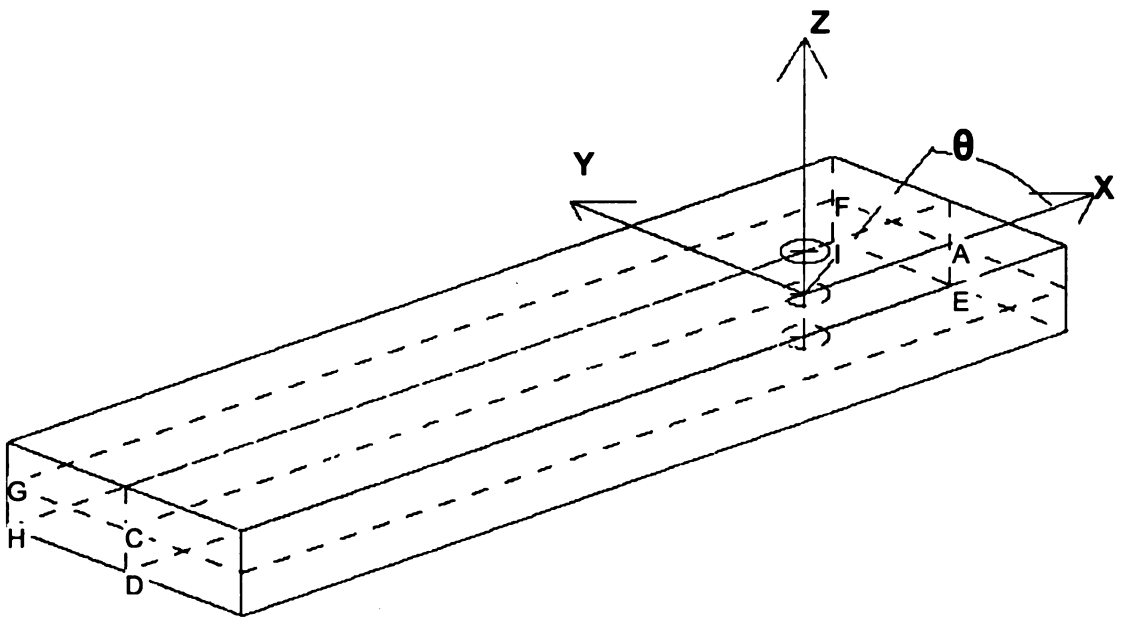

Figure 13 - The coordinate system established for problem modeling.

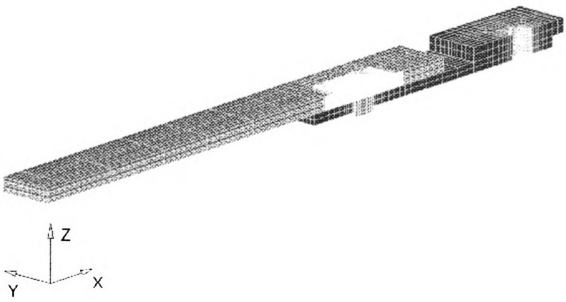

Figure 14 - The model in the finite element analysis (quarter of components in Figure 1).

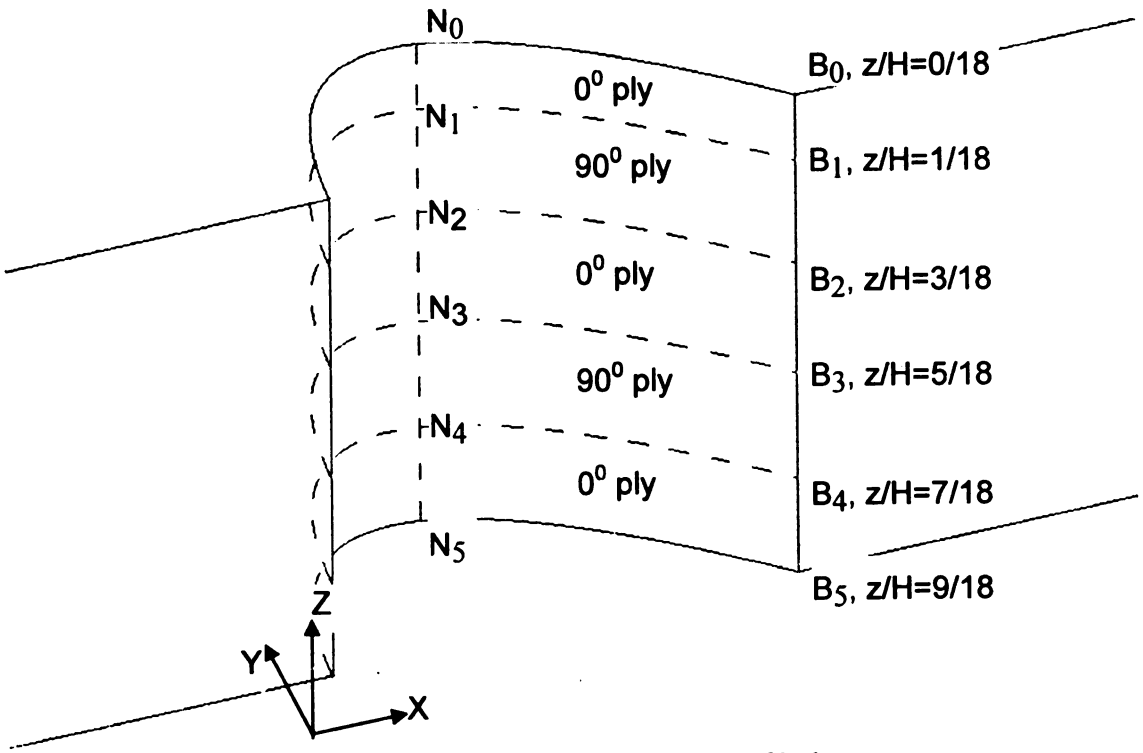

Figure 15 - A Schematic diagram of hole area on the composite plate.

The points B_5 and N_5 are located on the surface of the composite laminate. Hence, the Z/H ratios for both B_5 and N_5 are 0.5. Similarly, B_1, B_2, B_3, and B_4 are located at $\theta = 0^0$ but different Z positions while N_1, N_2, N_3, and N_4 are located at $\theta = 90^0$ with Z positions identical to the corresponding B_n points.

The composite laps investigated in this study were considered to behave linearly up to catastrophic failure. For the case H/D= 1, an ultimate force of 5.23 kN was used in the finite element simulation. This force was based on the testing results of Chapter 3. Since only one quarter of the mechanical fastener was modeled in the study, only 1.308 kN was required in the finite element simulation. Proportionally, 2,616N was required for the case H/D= 0.5 and 654N was required for the case H/D= 2.

The finite element analysis was based on the commercial code ABAQUS 6.3. Eight-noded brick elements were used as the building brick of the finite element model. Since the stress states on the hole surface and its vicinity were of primary interest, very fine meshes were used in these areas. Figure 16 shows the details of composite hole area in the finite element model. In the X-Y plane, there were 60 elements around the circumference of the half hole from B_n to N_n. In the thickness direction, 27 layers of element were modeled, resulting in six layers of element for each composite ply.

The contact between the composite laminate and the elastic pin and between the composite laminate and the steel lap were modeled using the contact pair approach in ABAQUS. The contact pair approach was selected for its simplicity. It was based on a master-slave concept, and the contact problem was solved with the Lagrange multiplier method. Since the movement between joint components was expected to be small, the

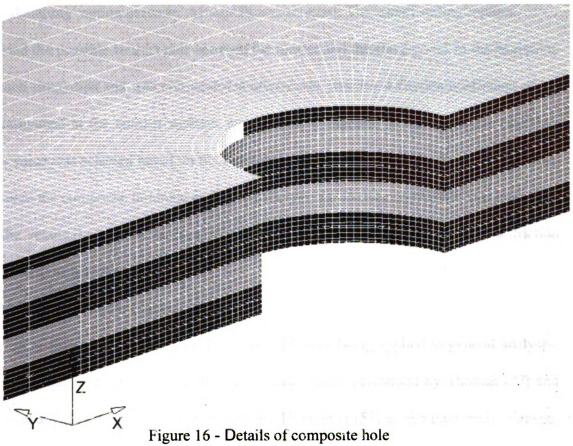

Figure 16 - Details of composite hole area in the finite element model.

'small sliding' option given by ABAQUS was selected. The 'small sliding' option defined the possible contact pair between the master and the slave nodes in the beginning of each simulation and was not redefined afterwards. Besides, a friction coefficient of 0.2 was assumed at the contact surfaces between the composite laminate and the steel lap. This value was selected based on the measurements by Blom [89]. On the contact surface between the composite laminate and the elastic pin, the friction coefficient was lower due to the relatively smooth surface of the pin and the hole surface. Hence, a friction coefficient of 0.1 was used.

C. Validation of Finite Element Analysis

Finite element modeling must be validated before being applied to general analyses. Experimental investigations based on strain gages were performed by Thomas [27] and Hung et al [55] for finite element validations. Hung et al [55] used a progressive damage model to predict the response of the pinned and clamped joints. Although the nearest strain gauge was only one hole radius from the hole edge, it was too far from where the failure took place, i.e. the hole edge. In his study, Tomas [27] mounted strain gauges 2.5mm from the edge of a hole with a diameter of 6mm. The comparisons between the measured and the calculated strains were inconclusive. The difficulties in both studies were believed to be attributed to the high gradients of strain around the hole edges.

In addition to experiments, validated computational results available in literatures were often used for justifications of new finite element modeling. Mahmood, Shokrieh and Lessard [32] studied the stress states of pin-joined composite structures with a finite element code developed by them. Radial displacement boundary conditions were applied to the nodes on the hole surfaces in their study rather than the aforementioned contact

pair approach, which was more computationally demanding. No friction between the pin and the hole was included in their study. In the present study, Lessard and Mahmood's studies were repeated with the use of ABAQUS and the contact pair approach to justify the proposed finite element model.

Cross-ply composite laminates with stacking sequences of $[0_4/90_4]_S$ and $[90_4/0_4]_S$ were investigated by both finite element codes, the Mahmood-Shokrieh-Lessard's and ABAQUS. The finite element mesh used by Mahmood, Shokrieh and Lessard was also adopted. Figure 17 shows the comparisons along the interface between the top two layers of the $[0_4/90_4]_S$ laminate, i.e. the interface between lamina 0_4 and lamina 90_4, at the hole edge. It is clear that the stress values from both studies agree with each other well at $\theta=0^o$ and $\theta=90^o$, where the stress values were believed to be most influential to the joint failures due to the potential bearing and net-section damage modes, respectively. Another study on $[90_4/0_4]_S$ laminate also concluded the good agreement at $\theta=0^o$ and $\theta=90^o$ based on the two approaches.

For the areas between $\theta=0^o$ and 90^o, Mahmood-Shokrieh-Lessard's study and the present approach predicted similar trends. The present approach, however, gave higher values of longitudinal compression σ_{xx} while lower values of other stress components than those given in Reference [32]. The discrepancies were believed to be attributed to the difference of boundary conditions used in simulations. In Mahmood-Shokrieh-Lassard's study, the assigned radial displacement around a section of the hole periphery without friction implied a rigid, frictionless pin. In the present study, however, contact condition was established between the hole surface and a rigid pin. The validation of the

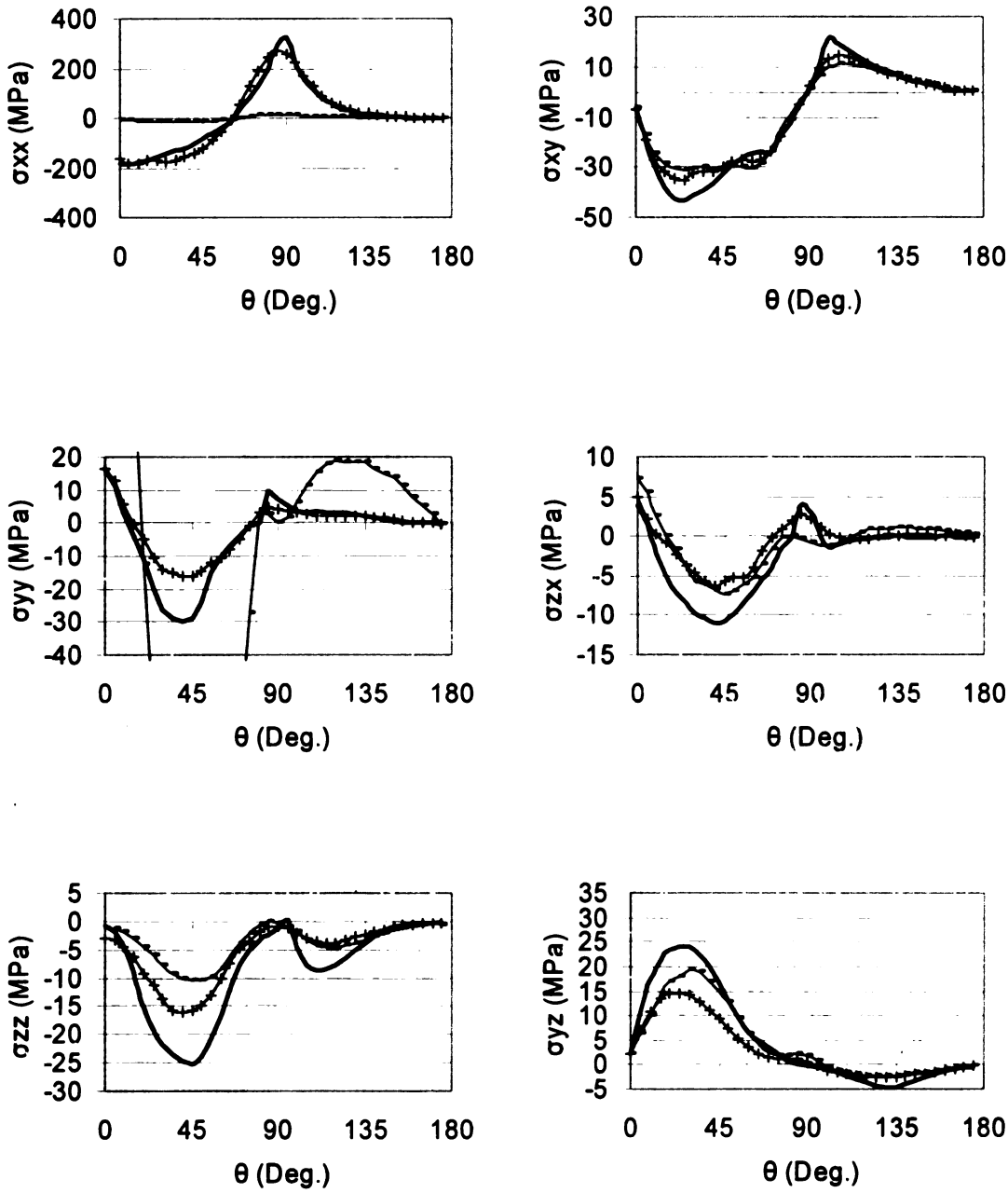

Figure 17 - Comparison of stress results between [32] and current model: **Bolt line**, [32]; '+' 0^0 ply results; '-' 90^0 ply results.

displacement distribution around the hole surface was also made. The result is shown in Figure 18.

4. 3 Finite Element Results

A. Three-dimensional Effect

The six stress components along line B_0-B_5 and line N_0-N_5, i.e. the bearing points and the net-section points through the half thickness of the composite laminate as depicted in Figure 15, respectively, are presented in Figure 19 and Figure 20, respectively. They are expressed in terms of the global XYZ coordinate system as shown in Figure 13 instead of the local material system of individual plies.

From Figure 19, it was clear that the stress distribution was non-uniform through the laminate thickness. It seemed most stress components reached the highest values at the laminate surface, i.e. B_5. For example, the longitudinal compressive stress σ_{XX} increased from 672MPa at B_0 to 962MPa at B_5 in the mid-plane of the innermost 0^o-ply B_0, i.e. the mid-plane of the composite laminate. That was an increase of 43%. The increase was 290% for σ_{yy}, transverse tensile stress from 52MPa at B_0 to 151MPa at B_5. The largest non-uniformity, however, was obviously seen in σ_{ZZ}, where it changed from -45MPa (compression) at B_0 to 75MPa (tension) at B_5. Among the three shear stress components, τ_{xy} , τ_{zx} and τ_{yz}, τ_{zx} took the highest value, around 60MPa, as well as highest level of non-uniformity, ranging from 0 at B_0 to -37MPa at B_5.

There were two 90^o plies in the half thickness. The stress distributions in these two 90^o plies were not uniform either. Figure 19 shows that σ_{XX} ranged from -152 to

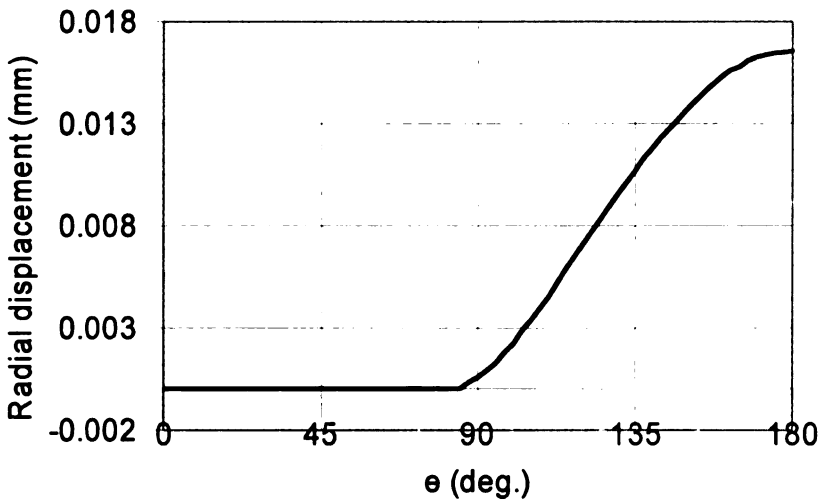

Figure 18 - ABAQUS result of radial displacement on the hole periphery of $[0_4/90_4]_S$ cross-ply

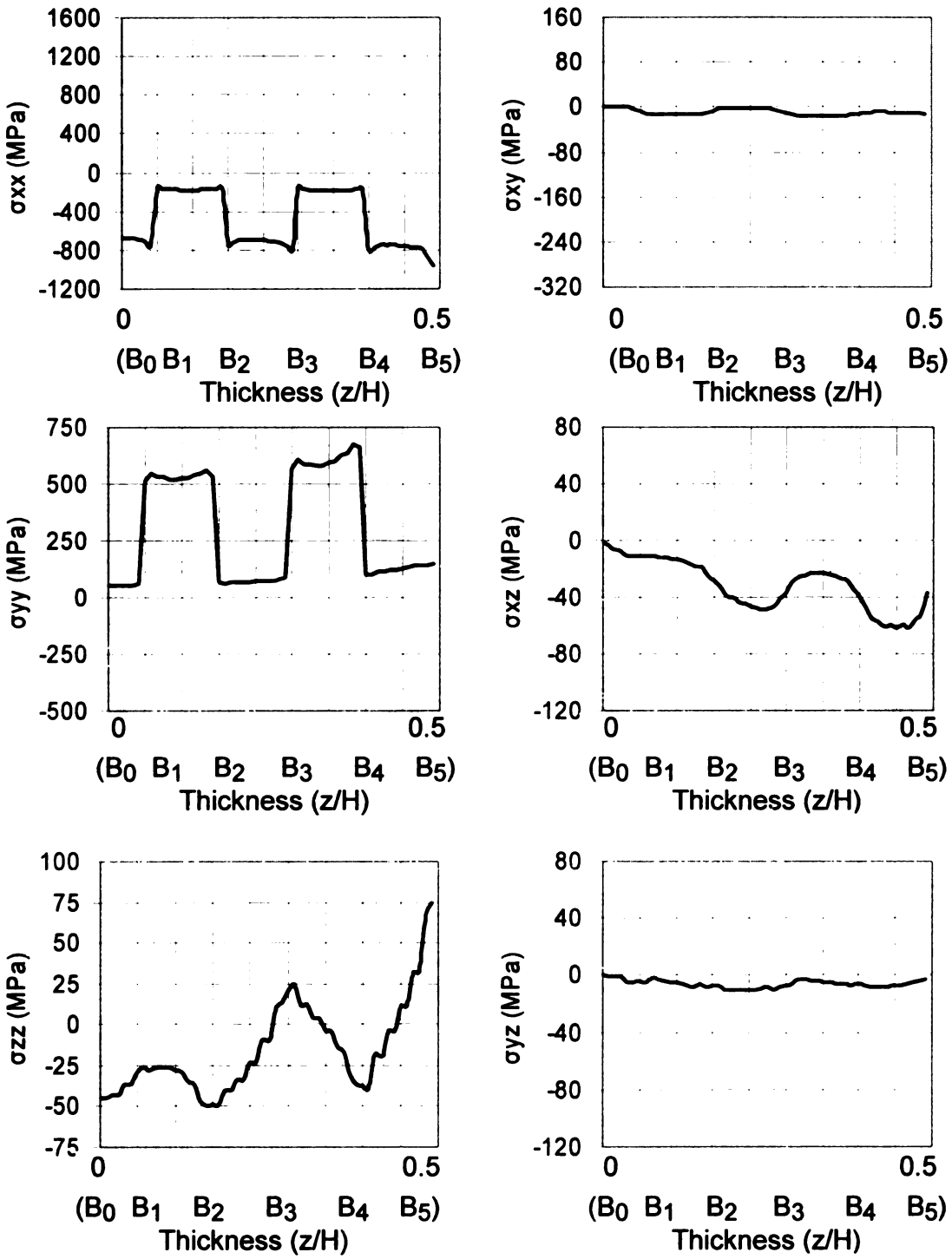

Figure 19 - H/D=1 stress state through the thickness at B_0-B_5 line.

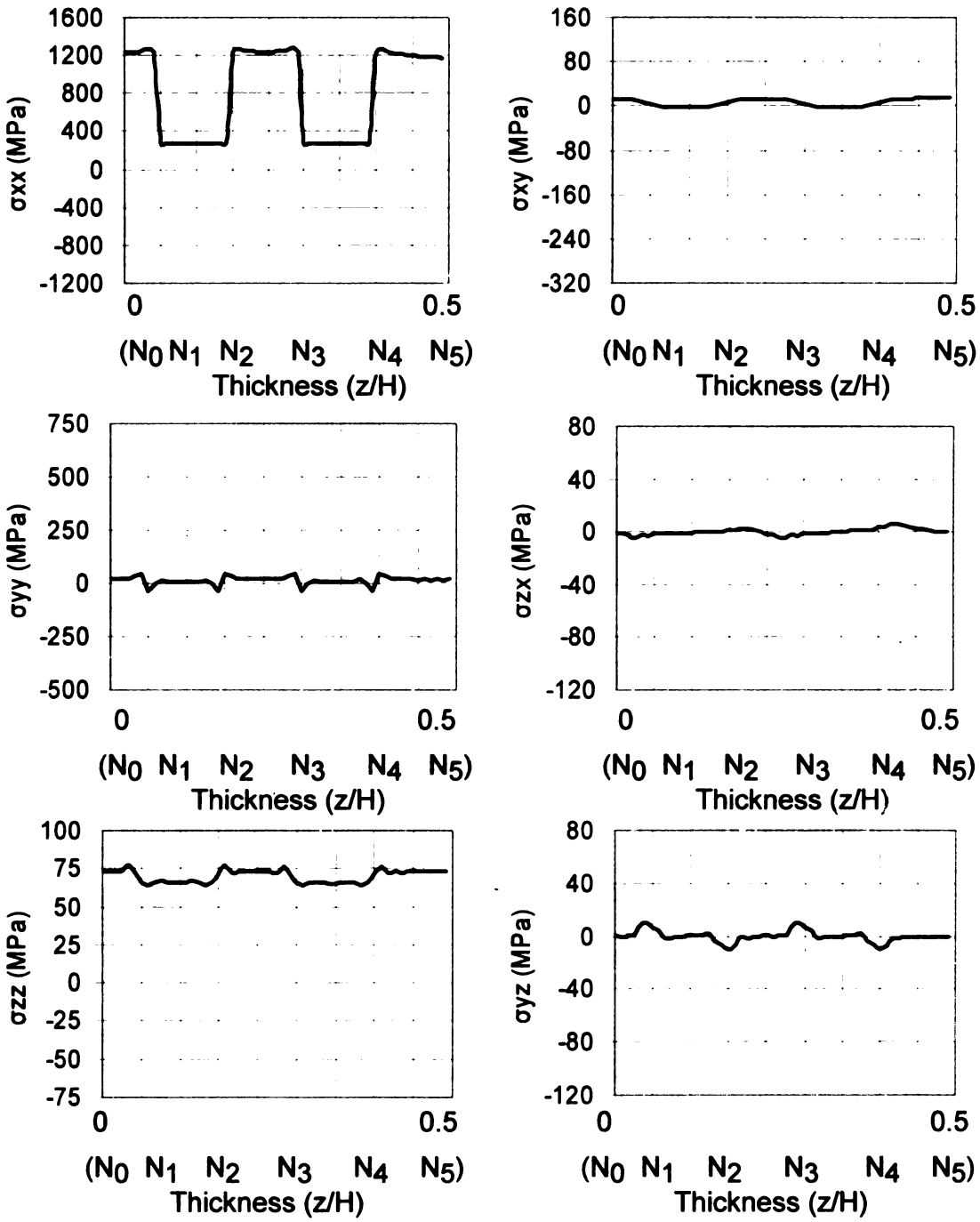

Figure 20 - H/D=1 stress state through the thickness at N_0-N_5 line.

-180MPa, σ_{yy} ranged from 522 to 662MPa, σ_{zz} ranged from -50 to 25MPa and τ_{zx} ranged from -11 to -40MPa.

Comparisons between Figure 19 and Figure 20 revealed that the stress distribution along line N_0-N_5 was much more uniformly distributed through the thickness than along line B_0-B_5. The longitudinal tensile stress σ_{xx} valued 1231MPa at B_0 and 1177MPa at B_5. That was a variation less than 5%. The variation of the transverse normal stress σ_{yy} was only 3%, from 18.8MPa at B_0 to 18.3MPa at B_5. However, σ_{zz} remained positive (tension) throughout the thickness and valued almost equally from N_0 to N_5.

B. Size Effect

Figure 21 shows the stress distributions at the bearing point through the half thickness of the laminates for cases H/D= 0.5 (cross line), H/D= 1 (solid line), and H/D= 2 (dash line). They had similar trends and were all non-uniform through the laminate thickness. Comparisons of the three cases also revealed that case H/D= 0.5 bore the least non-uniformity whereas case H/D= 2 the highest non-uniformity. The increase in longitudinal compressive stress σ_{xx} from B_0 to B_5 for case H/D= 0.5 was 17%, i.e. from -713 to -835MPa. It was 43% for case H/D= 1, from -672 to -962MPa, and 343% for case H/D= 2, from -476 to -1632MPa. The increase in the transverse tensile stress σ_{yy} from B_0 to B_5 for case H/D= 0.5 was 68%, i.e. from 56 to 94MPa. It was 290% for case H/D= 1, from 52MPa at B_0 to 151MPa, and 536% for case H/D= 2, from 61 to 327MPa. The through-

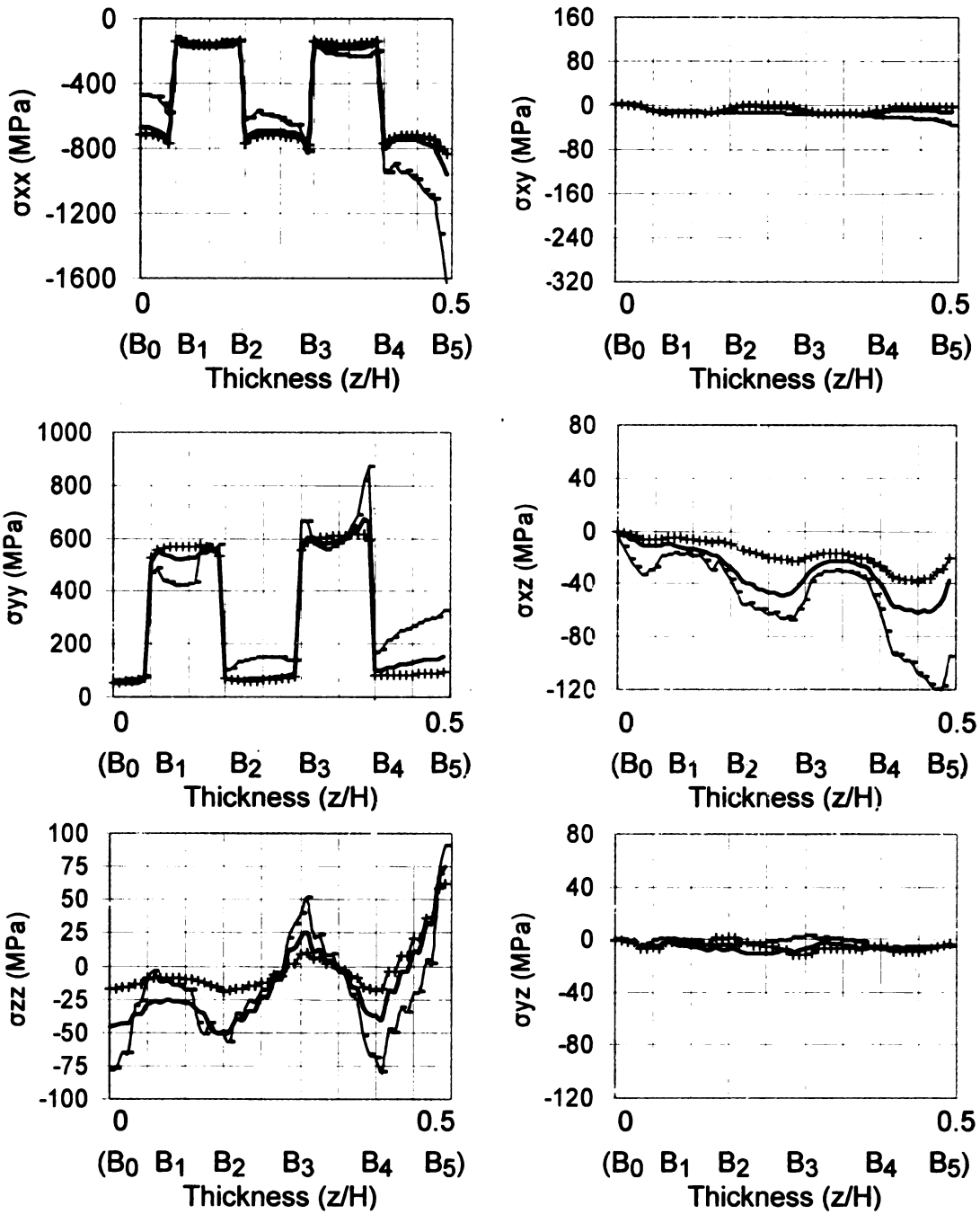

Figure 21 – Stress comparison of H/D=1/2 (cross line), 1 (solid line) and 2 (dash line) cases at B_0-B_5 line.

the-thickness normal stress σ_{ZZ} changed from -17MPa at B_0 to 62MPa at B_5 for case H/D= 0.5. It changed from -45MPa at B_0 to 75MPa at B_5 H/D= 1 and from -78MPa at B_0 to 91MPa at B_5 for case H/D= 2. The variation of transverse shear stress τ_{ZX} from B_0 to B_5 was from 0 to -21MPa for case H/D= 0.5, from 0 to -37MPa for case H/D= 1, and from 0 to -95MPa for case H/D= 2.

Similarly, as the ratio H/D became larger, i.e. from 0.5 to 1 and to 2, the non-uniformity of stress distributions in 90° plies became higher. Along line B_0-B_5, the variation of σ_{XX} was from 1260MPa at B_0 to 1201MPa at B_5 for case H/D= 0.5. It was from 1231MPa at B_0 to 1177MPa at B_5 for case H/D= 1 and from 1,093MPa at B_0 to 1267MPa at B_5 for case H/D= 2. The variation range in σ_{YY} from B_0 to B_5 was from 21.9 to 18.4MPa for case H/D= 0.5, from 18.8 to 18.4MPa for H/D=1 model, and from 17.4 to 19.8MPa for H/D= 2, The variations of σ_{ZZ} from B_0 to B_5 for cases H/D= 0.5, 1 and 2 are from 58.7 to 58.5MPa, from 73.5 to 73.4MPa, and from 74.1 to 62.9MPa, respectively.

C. Comparisons with Experiments

As discussed in section A in this Chapter, the stress state around the hole not only varied along the hole periphery in the X-Y plane, but also varied through the laminate thickness. Only a three-dimensional study, as opposed to two-dimensional plane-strain or plane-stress study, could possibly reveal these responses. The finite element analysis revealed that the bearing line, from B_0 to B_5, had the highest non-uniformity along the hole periphery. The surface point B_5, in most cases, had the highest stress along the laminate thickness. This result seemed to indicate that the non-uniform stress distribution

through the laminate thickness was caused by the bending of pin which and associated indentations had been observed in experiments.

The three-dimensional stress study could also provide out-of-plane stress components. In the case H/D= 1, the out-of-plane normal stress σ_{ZZ} amounted up to 75MPa, which was about 7.8% of the longitudinal compressive stress σ_{XX}, i.e. 962MPa, at B_5. Moreover, σ_{ZZ} switched its sign from negative in the inner plies to positive in the outer plies. Since positive σ_{ZZ} could cause matrix cracking and delamination, it indicated that the outer plies were more vulnerable to these types of failure than the inner plies. Experimental results verified this argument. Besides, the out-of-plane shear stress τ_{ZX} also valued 37MPa, which was about 51% of the shear strength (S_{ZX} was equals to 72MPa for the composite studied.), at the outer ply of the composite laminate. Hence, it seemed that the out-of-plane stresses should be involved in all composite failure analysis.

The previous section concluded that when the geometric ratio H/D increased from 0.5 to 1 and to 2, the level of non-uniformity also increased. As observed in experiments in Chapter 2, a larger H/D ratio would result in a "tighter" contact and more localized damage in the area close to laminate surface, such as B_5.

4. 4 Failure Analysis

A. One-Parameter Failure theory

Once the stress distributions were obtained, they could be substituted into a failure criterion to evaluate the status of a composite joint. This process was especially useful for

failure criteria based on material strengths and the point with the most critical stress.The many failure criteria available in the literature could be divided into the following three categories: global failure criteria, fiber-buckling failure criteria, and micro-mechanical failure criteria.

A. 1 Global Failure Criteria

The maximum stress failure criterion for composite materials is similar to those used for isotropic materials which were based on maximum normal stress or maximum shear stress proposed by Rankine and Tresca, respectively. Based on the maximum stress criterion, the composite failure is predicted in the lamina level. If any of the normal or shear stress of a composite lamina reaches the corresponding ultimate strength, the composite lamina, and hence the composite joint, is considered to fail. Instead of using the stress components individually in the maximum stress criterion, Tsai-Hill [90] proposed a failure theory which was based on the combination of individual stress components. In their theory, a lamina will fail when the distortion energy of it is greater than the allowable level. Tsai-Wu [91] refined the Tsai-Hill theory by distinguishing the compressive stress from the tensile stress in a lamina. Maximum stress, Tsai-Hill and Tsai-Wu failure theories could be represented by equation (1-3) respectively.

Maximum Stress Failure Criterion

$Maximum(e_{max\_xx}, e_{max\_yy}, e_{max\_zz}, e_{max\_xy}, e_{max\_yz}, e_{max\_zx}) = e_{max}$

Where,

$$\text{for}\sigma_{xx} > 0, e_{max\_xx} = \frac{\sigma_{xx}}{X_T}$$

$$\text{for}\sigma_{xx} < 0, e_{max\_xx} = \frac{\sigma_{xx}}{X_C}$$

$$\text{for}\sigma_{yy} > 0, e_{max\_yy} = \frac{\sigma_{yy}}{Y_T}$$

$$\text{for}\sigma_{yy} < 0, e_{max\_yy} = \frac{\sigma_{yy}}{Y_C}$$

$$\text{for}\sigma_{zz} > 0, e_{max\_zz} = \frac{\sigma_{zz}}{Y_T}$$

$$\text{for}\sigma_{zz} < 0, e_{max\_zz} = \frac{\sigma_{zz}}{Y_C}$$

$$e_{max\_xy} = \left|\frac{\sigma_{xy}}{S_{xy}}\right|, \; e_{max\_yz} = \left|\frac{\sigma_{yz}}{S_{yz}}\right|, \; e_{max\_xy} = \left|\frac{\sigma_{zx}}{S_{zx}}\right| \qquad (1)$$

Tsai-Hill Failure Criterion

$$\left(\frac{\sigma_{xx}}{X_T}\right)^2 + \left(\frac{\sigma_{yy}}{Y_T}\right)^2 + \left(\frac{\sigma_{zz}}{Y_T}\right)^2 - 2G_{xyTH}\sigma_{xx}\sigma_{yy} - 2G_{zxTH}\sigma_{zz}\sigma_{xx} - 2G_{yzTH}\sigma_{yy}\sigma_{zz}$$

$$+\left(\frac{\sigma_{xy}}{S_{xy}}\right)^2 + \left(\frac{\sigma_{zx}}{S_{zx}}\right)^2 + \left(\frac{\sigma_{yz}}{S_{yz}}\right)^2 = e_{TH}{}^2$$

Where,

$$\sqrt{\frac{1}{G_{xyTH} + G_{zxTH}}} = X_T$$

$$\sqrt{\frac{1}{G_{zxTH} + G_{yzTH}}} = Y_T$$

$$\sqrt{\frac{1}{G_{yzTH} + G_{xyTH}}} = Y_T \qquad (2)$$

Tsai - Wu Failure Criterion

$$\frac{\sigma_{xx}}{X_{xTW}}+\frac{\sigma_{yy}}{Y_{yTW}}+\frac{\sigma_{zz}}{Y_{zTW}}+(\frac{\sigma_{xx}}{X_{xxTW}})^2+(\frac{\sigma_{yy}}{Y_{yyTW}})^2+(\frac{\sigma_{zz}}{Y_{zzTW}})^2+$$

$$\frac{2\sigma_{xx}\sigma_{yy}}{X_{xyTW}}+\frac{2\sigma_{zz}\sigma_{xx}}{X_{zxTW}}+\frac{2\sigma_{yy}\sigma_{zz}}{X_{yzTW}}+(\frac{\sigma_{xy}}{S_{xyTW}})^2+(\frac{\sigma_{zx}}{S_{zxTW}})^2+(\frac{\sigma_{yz}}{S_{yzTW}})^2=e_{TW}{}^2$$

Where,

X_{xTW}, Y_{yTW}, Y_{zTW}, X_{xxTW}, Y_{yyTW}, Y_{zzTW}, S_{xyTW}, S_{xyTW} and S_{xyTW}

could be solved by theoretical single stress cases, and by assuming

$$\begin{aligned} X_{xyTW} &= 2(X_T)^2 \\ X_{zxTW} &= 2(X_T)^2 \\ X_{yzTW} &= 2(Y_T)^2 \end{aligned} \qquad (3)$$

A. 2 Fiber-buckling Failure Criteria

In a micromechanical study concerning the compressive failure of fiber composites, Argon [92] identified that the shear yielding stress of a composite κ, which was equal to the multiplication of shear modulus G_{xy} and yielding shear strain γ_y, and an initial fiber misalignment angle ϕ_0 as the main parameters controlling the compressive strength of the composite. Equation (4) shows the Argon theory,

for $\sigma_{XX} < 0$ $$\frac{\sigma_{xx}}{\frac{G_{xy}\bullet\gamma_y}{\phi_0}}=e_{argon} \qquad (4)$$

where G_{xy} is shear modulus and γ_y is yielding shear strain. The composite is considered to have failed when e_{argon} reaches 1. In the Argon theory, the material was considered to be rigid perfectly plastic. Budiansky [93] extended Argon's formula by assuming the material to be elastic perfectly plastic. His prediction of critical compressive stress is shown in Equation (5).

$$\text{for } \sigma_{xx} < 0 \qquad \frac{\sigma_{xx}}{\dfrac{G_{xy} \bullet \gamma_y}{\phi_0 + \gamma_y}} = e_{budi} \tag{5}$$

Both the Argon theory and the Budiansky theory accounted for fiber micro-buckling or fiber kinking failure typically seen in polymer-matrix composite under compression.

A. 3 Micro-mechanical Failure Criteria

Yamada and Sun [94] proposed a failure criterion accounting for lamination effect. The shear strength in their criterion was proposed to be measured from a symmetric cross-ply laminate instead of a unidirectional specimen. The Yamada-Sun theory is given in Equations (6a) and (6b) accounting for the failure mode combining fiber tension (breakage) and shear and the failure mode combining fiber compression (buckling) and shear, respectively,

$$\text{for } \sigma_{xx} > 0 \qquad (\frac{\sigma_{xx}}{X_t})^2 + (\frac{\tau_{xy}}{S_{xy}})^2 = e_{ft}^{\ 2} \tag{6a}$$

$$\text{for } \sigma_{xx} < 0 \qquad (\frac{\sigma_{xx}}{X_c})^2 + (\frac{\tau_{xy}}{S_{xy}})^2 = e_{fc}^{\ 2} \tag{6b}$$

where X_t and X_c are tensile and compressive strengths of unidirectional composite lamina along the fiber direction and S_{xy} is the in-plane shear strength of a symmetric cross-ply laminate. Hashin [43] included matrix tension and compression in his failure criterion. His matrix related failure theory is given in Equations (7a) and (7b) to differentiate the failure mode combining matrix tension and shear and the failure mode combining matrix compression and shear, respectively,

for $\sigma_{yy} > 0$ $$(\frac{\sigma_{yy}}{Y_t})^2 + (\frac{\tau_{xy}}{S_{xy}})^2 = e_{mt}^{\ 2} \tag{7a}$$

for $\sigma_{yy} < 0$ $$(\frac{\sigma_{yy}}{Y_c})^2 + (\frac{\tau_{xy}}{S_{xy}})^2 = e_{mc}^{\ 2} \tag{7b}$$

where Y_t and Y_c are tensile and compressive strengths of unidirectional composite lamina along the matrix direction. Puck [95] put a major emphasis on matrix failure in three-dimensional cases by including interlaminar composite failure, such as delamintation, in his failure criterion shown in Equations (8a) and (8b),

for $\sigma_{zz} > 0$ $$(\frac{\tau_{zx}}{S_{zx}})^2 + (\frac{\tau_{yz}}{S_{yz}})^2 + (\frac{\sigma_{zz}}{Y_t})^2 = e_{puck}^{\ 2} \tag{8a}$$

for $\sigma_{zz} < 0$ $$(\frac{\tau_{zx}}{S_{zx}})^2 + (\frac{\tau_{yz}}{S_{yz}})^2 + (\frac{\sigma_{zz}}{Y_c})^2 = e_{puck}^{\ 2} \tag{8b}$$

where S_{zx} and S_{yz} are interlaminar strengths.

B. Comparisons of One-Parameter Failure Criteria

As given in Table 9 are the effective status values, or failure indicators, based on all failure criteria presented in the previous section for point B_5 of case H/D= 1. When an effective value is equal to or greater than 1, it implies that failure will take place at the point according to the damage mode specified by the equation; otherwise the point remains intact. Hashin's tensile matrix failure e_{mt} took a value of 4.87, comparing to 0.18 for e_{mc} , 0.18 for e_{ft} and 1.1 for e_{fc}. It could be inferred from these values that tensile matrix failure beneath the pin occurred at a much earlier stage than the ultimate failure of the composite joint. In other words, the composite joint could still withstand a higher load beyond the occurrence of tensile matrix failure.

The out-of-plane failure indicator e_{puck} had a value of 2.47. It also indicated that the local out-of-plane failure beneath the pin would not dictate the load capacity of the composite joint. Nevertheless, the matrix cracking and out-of-plane buldging could be easily identified in the damaged specimens. On the contrary, the values of the indicators, e_{fc}= 1.11, e_{argon}= 1.10 and e_{budi}= 1.41, seemed to indicate that a compressive fiber failure was the primary failure mode of the composite joint. Taken into account that both Argon's and Budiansky's theories were aimed at fiber micro-buckling or fiber kinking failure typically seen in polymer-matrix composites under compression, it would be logical to predict that these types of failure mode would take place in failed specimens. In fact, in Chapter 3, zig-zag kinks were reported in the bearing area of failed composite joints.

Table 9 – Failure indicators at B_0-B_5 line.

		e_{max}	e_{TH}^2	e_{TW}^2	e_{argon}	e_{budi}	e_{ft}	e_{fc}	e_{mt}	e_{mc}	e_{puck}
H/D=1/2											
B_0 (0^o)		1.80	2.03	3.55	0.81	1.05	0.03	0.81	1.80	0.03	0.15
B_1	0^o	2.24	3.93	4.58	0.88	1.13	0.07	0.88	2.24	0.07	0.31
	90^o	1.23	19.66	1.2	0	0	0.56	0.11	0.11	1.24	0.26
B_2	90^o	1.23	17.82	0.10	0	0	0.57	0.11	0.11	1.24	0.38
	0^o	2.23	3.38	4.94	0.87	1.12	0.08	0.87	2.29	0.08	0.23
B_3	0^o	2.56	7.22	4.71	0.89	1.15	0.09	0.89	2.56	0.09	0.56
	90^o	1.21	19.61	4.92	0	0	0.59	0.12	0.12	1.22	0.88
B_4	90^o	1.23	17.98	0.68	0	0	0.63	0.14	0.14	1.23	0.96
	0^o	2.74	5.43	6.25	0.87	1.13	0.11	0.88	2.74	0.11	0.45
B_5 (0^o)		3.02	1.74	2.25	0.95	1.23	0.05	0.95	3.02	0.05	2.04
H/D=1											
B_0 (0^o)		1.67	0.46	4.49	0.77	0.99	0.03	0.76	1.67	0.03	0.38
B_1	0^o	2.04	1.37	5.30	0.86	1.10	0.07	0.86	2.04	0.07	0.40
	90^o	1.29	16.43	-1.69	0	0	0.54	0.11	0.11	1.30	0.50
B_2	90^o	1.31	12.57	-4.32	0	0	0.57	0.13	0.13	1.32	1.04
	0^o	2.20	1.14	6.83	0.85	1.10	0.09	0.86	2.20	0.09	0.64
B_3	0^o	2.86	7.06	4.83	0.92	1.19	0.12	0.93	2.86	0.12	0.80
	90^o	1.40	20.87	9.37	0	0	0.61	0.16	0.16	1.32	1.56
B_4	90^o	1.36	18.21	-0.91	0	0	0.71	0.20	0.20	1.37	1.38
	0^o	3.33	5.52	10.16	0.91	1.17	0.18	0.92	3.34	0.18	0.70
B_5 (0^o)		4.87	7.17	3.15	1.10	1.41	0.18	1.11	4.87	0.18	2.47
H/D=2											
B_0 (0^o)		1.97	0.47	7.51	0.54	0.70	0.0	0.54	1.97	0.0	0.66
B_1	0^o	2.41	2.88	5.64	0.66	0.85	0.12	0.67	2.41	0.12	0.50
	90^o	1.05	14.65	1.1	0	0	0.51	0.15	0.15	1.06	1.06
B_2	90^o	1.16	9.15	-4.19	0	0	0.63	0.21	0.21	1.18	1.23
	0^o	3.31	3.39	11.26	0.70	0.90	0.20	0.73	3.32	0.20	0.72
B_3	0^o	4.45	13.16	6.81	0.93	1.20	0.26	0.97	4.46	0.26	1.34
	90^o	2.03	22.95	17.22	0	0	0.73	0.26	0.26	1.49	2.34
B_4	90^o	1.88	24.53	-3.33	0	0	0.96	0.33	0.33	1.78	1.97
	0^o	5.32	11.14	25.12	1.07	1.38	0.33	1.12	5.33	0.33	1.09
B_5 (0^o)		10.54	62.47	16.83	1.86	2.39	0.53	1.93	10.56	0.53	3.24

In Table 10, e_{puck} at N_0, N_1 ... and N_5 also revealed that out-of-plane failure would not dictate the load capability. However, e_{ft} at N_0, N_1 ... and N_5 were all higher than 1. This fact indicates that at net-section plane, net-section failure is also a potential failure model competing against bearing failure.

C. Two-Parameter Failure Analysis

As discussed earlier, a two-parameter failure model is useful because it does not underestimate the joint strength as the one-parameter counterparts and is simpler than the progressive counterparts in failure prediction. Based on the foregoing detailed computations for both in-plane stresses and through-the-thickness stresses, it is possible to develop a two-parameter failure model by introducing a characteristic dimension in the thickness direction, i.e. away from the laminate outer surface.

Based on the previous studies in both Chapters 2 and 3, the stresses along laminate surface, i.e. along line B_5-S_5 as depicted in Figure 22(a), and along the 45° line from the mid-plane of the composite laminate to the laminate surface, i.e. line B_0-S_5, were also of interest. More finite element simulations were carried out for the points along these lines, each focusing on one point along the three edges of the triangle zone given in Figure 22(a). The failure criteria presented earlier were also used for calculating the load capacity of the composite joint. The results are given in Table 11. For example, C_{ft} stands for the load capability based on the Yamada-Sun fiber tension failure criterion.

Table 10 – Failure indicators at N_0-N_5 line.

		e_{max}	e_{TH}^2	e_{TW}^2	e_{argon}	e_{budi}	e_{ft}	e_{fc}	e_{mt}	e_{mc}	e_{puck}
H/D=1/2											
N_0 (0°)		1.89	3.03	3.31	0	0	1.31	0.15	0.72	0.15	1.89
N_1	0°	1.89	1.87	2.93	0	0	1.28	0.08	1.47	0.08	1.94
	90°	8.69	49.50	13.84	0.04	0.06	0.06	0.07	8.69	0.06	1.66
N_2	90°	8.68	49.35	13.82	0.04	0.06	0.06	0.07	8.68	0.06	1.66
	0°	1.88	1.86	2.92	0	0	1.28	0.08	1.47	0.08	1.93
N_3	0°	1.88	1.85	2.91	0	0	1.28	0.08	1.46	0.08	1.93
	90°	8.63	48.81	13.70	0.04	0.06	0.06	0.07	8.63	0.06	1.65
N_4	90°	8.53	47.23	13.24	0.04	0.06	0.06	0.08	8.53	0.06	1.66
	0°	1.89	1.83	2.87	0	0	1.26	0.09	1.44	0.09	1.94
N_5 (0°)		1.89	3.15	3.25	0	0	1.26	0.19	0.62	0.19	1.89
H/D=1											
N_0 (0°)		2.37	4.66	3.91	0	0	1.29	0.19	0.64	0.19	2.37
N_1	0°	2.31	2.39	3.05	0	0	1.28	0.09	1.45	0.09	2.34
	90°	8.87	45.42	11.08	0.04	0.05	0.05	0.06	8.87	0.05	2.14
N_2	90°	8.89	45.65	11.16	0.04	0.05	0.05	0.06	8.89	0.05	2.13
	0°	2.31	2.38	3.05	0	0	1.29	0.09	1.45	0.09	2.34
N_3	0°	2.30	2.37	3.06	0	0	1.29	0.08	1.45	0.08	2.33
	90°	8.91	46.12	11.31	0.04	0.05	0.05	0.06	8.91	0.05	2.12
N_4	90°	8.85	45.31	11.12	0.04	0.05	0.05	0.06	8.85	0.05	2.12
	0°	2.29	2.35	3.03	0	0	1.28	0.08	1.44	0.08	2.32
N_5 (0°)		2.37	4.57	3.79	0	0	1.24	0.22	0.63	0.22	2.37
H/D=2											
N_0 (0°)		2.39	4.57	3.66	0	0	1.15	0.22	0.60	0.22	2.39
N_1	0°	2.22	2.23	2.84	0	0	1.12	0.10	1.30	0.10	2.24
	90°	8.39	40.15	10.16	0.03	0.04	0.06	0.06	8.39	0.06	2.10
N_2	90°	8.60	42.82	10.73	0.03	0.04	0.06	0.06	8.60	0.06	2.06
	0°	2.23	2.23	2.88	0	0	1.28	0.10	1.34	0.10	2.24
N_3	0°	2.21	2.42	3.15	0	0	1.31	0.09	1.39	0.09	2.25
	90°	9.24	52.33	13.46	0.03	0.04	0.04	0.05	9.24	0.04	2.14
N_4	90°	9.68	60.00	15.48	0.03	0.04	0.03	0.04	9.68	0.03	1.94
	0°	2.09	2.29	3.20	0	0	1.39	0.08	1.45	0.08	2.12
N_5 (0°)		2.03	3.61	3.58	0	0	1.33	0.22	0.68	0.22	2.03

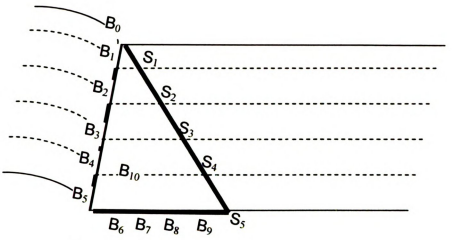

22(a).

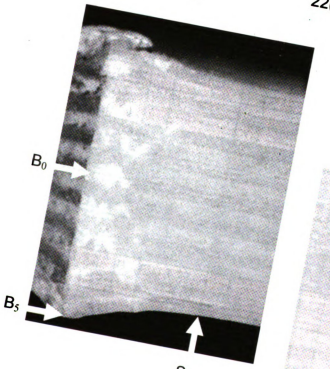

22(b).

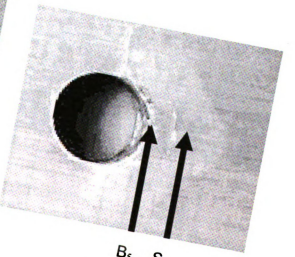

22(c).

Figure 22 – Two-parameter failure model triangle 22(a) and Front 22(b). Top 22(c) view of a failed sample in Chapter 3

Table 11 – Joint load capacity prediction .

B_0	C_{mt} 3.04														
	C_{budi} 5.31														
	C_{fc} 6.88														
	C_{puck} 12.88														
B_{1-}	C_{mt} 2.51	S_{1-}	C_{mt} 3.76												
	C_{budi} 4.71		C_{budi} 5.19												
	C_{fc} 6.09		C_{fc} 6.65												
	C_{puck} 11.61		C_{puck} 20.71												
B_{1+}	C_{mc} 4.01	S_{1+}	C_{mc} 4.43												
	C_{puck} 9.80		C_{ft} 13.61												
	C_{ft} 9.84		C_{puck} 21.95												
B_{2-}	C_{mc} 3.95			S_{2-}	C_{mc} 5.06										
	C_{puck} 5.07				C_{puck} 7.61										
	C_{ft} 9.31				C_{ft} 20.79										
B_{2+}	C_{mt} 2.32			S_{2+}	C_{budi} 5.92										
	C_{budi} 4.76				C_{fc} 7.58										
	C_{fc} 6.15				C_{mt} 9.07										
	C_{puck} 8.08				C_{puck} 20.41										
B_{3-}	C_{mt} 1.77					S_{3-}	C_{budi} 6.56								
	C_{budi} 4.40						C_{fc} 8.36								
	C_{fc} 5.65						C_{mt} 12.86								
	C_{puck} 6.51						C_{puck} 35.77								
B_{3+}	C_{puck} 3.42					S_{3+}	C_{mc} 5.79								
	C_{mc} 3.94						C_{puck} 24.22								
	C_{ft} 8.74						C_{ft} 25.74								
B_{4-}	C_{mc} 3.79								S_{4-}	C_{mc} 6.12					
	C_{puck} 3.85									C_{puck} 6.97					
	C_{ft} 7.39									C_{ft} 25.72					
B_{4+}	C_{mt} 1.52	B_{10}	C_{mt} 3.21						S_{4+}	C_{budi} 7.47					
	C_{budi} 4.47		C_{budi} 5.00							C_{mt} 9.45					
	C_{fc} 5.69		C_{fc} 6.40							C_{fc} 13.53					
	C_{puck} 7.28		C_{puck} 13.61							C_{puck} 23.69					
B_5	C_{mt} 1.03	B_6	C_{mt} 2.33	B_7	C_{mt} 4.86	B_8	C_{budi} 6.48	B_9	C_{budi} 7.31	S_5	C_{budi} 7.91				
	C_{puck} 2.20		C_{budi} 4.90		C_{budi} 5.75		C_{mt} 6.93		C_{mt} 8.82		C_{mt} 9.86				
	C_{budi} 3.71		C_{fc} 6.26		C_{fc} 7.33		C_{fc} 8.23		C_{fc} 9.25		C_{fc} 9.99				
	C_{fc} 4.73		C_{puck} 35.62		C_{puck} 33.47		C_{puck} 43.27		C_{puck} 61.32		C_{puck} 63.71				

The lowest value in Table 11 takes 1.03kN. It is for point B_5 with the use of Hashin's matrix tension failure criterion, i.e. C_{mt}. This value is well below the load capacity of 5.37kN from the experiment. Also, the predictions based on C_{puck}, C_{budi}, and C_{fc} at B_5 are all below 5.37KN, indicating that the composite joint at B_5 would fail before the true load capacity is reached if Puck's, Budiansky's and Yamada-Sun's failure theories are used. In other words, if B_5 is selected as the location to predict the load capacity for the composite joint, the joint strength would be underestimated no matter what failure theory is implemented. With the introduction of a characteristic dimension as suggested by the two-parameter failure criterion, it is possible to look for a neighboring point along line B_5-S_5 that may predict load capacity close to the true one. Following this approach and using 5.37kN as the benchmark, different failure theories would provide different characteristic dimensions. In fact, Puck's delamination theory and Yamada-Sun's fiber compression theory both yield a characteristic dimension below 0.32mm whereas Budiansky's fiber buckling theory and Hashin's matrix tensile theory give 0.48mm and 0.80mm as the characteristic dimension, respectively.

The characteristic dimension can also be obtained from the line B_5-B_0. Puck's delamination theory and Yamada-Sun's fiber compression theory both yield a characteristic dimension lower than 0.35mm while Hashin's matrix tensile theory does not yield a reasonable characteristic dimension lower than 1.65mm, i.e. half thickness of the composite laminate. Besides, Budiansky's theory gives a characteristic dimension of 1.62mm, fairly close to the half thickness of the laminate.

In identifying the characteristic length, the approach based on line B_0-B_5, i.e. along the laminate thickness, seems to indicate that the failure of the composite joint will not take place until the stress at point B_0 reaches the allowable level. On the contrary, the approach based on line B_5-S_5, i.e. along the laminate surface, seems to indicate that the failure of the composite joint will not take place until the stress at a point between B_6 and B_7 reaches the allowable level. Both approaches seem to be supported by the experimental results as shown in Figure 22(b) and 22(c), respectively. Another interesting correlation between computation and experiment can also be found from comparing Table 11 and Figure 22(b) and 22(c). In Table 11, the predicted values of load capacity below 5.37KN seem to be located around the left-lower corner while the damage in Figure 22(b) seems to be also primarily located around the left-lower area bounded by the triangle vertices B_0, B_5 and S_5.

4. 5 Conclusions

The following conclusions can be drawn from the foregoing investigations.

1. Three-dimensional stress analysis is critically important to the failure analysis of composite joints because the stress distribution around the composite joint is not only dependent on the in-plane (X-Y plane) dimensions but also dependent on the composite thickness. In addition, the out-of-plane stresses are not negligible when compared with the joint strength.
2. The geometrical ratio of composite joint H/D can greatly influence the stress non-uniformity through the composite thickness. The higher the ratio of H/D, the higher the non-uniformity.

3. The comparison of various failure theories can help to justify the suitability of the failure theories in predicting the strengths and failure modes of composite joints. It seems that Argon's theory, Budiansky's theory and Yamada-Sun's theories are the best ones to predict the strength and failure mode of the composite joint investigated.
4. Conventional two-parameter failure theories accounting for an in-plane characteristic dimension can be extended to account for a characteristic dimension in the thickness direction.

Chapter 5

Conclusions and Recommendations

5.1 Conclusions

A. Thickness, constraint and damage mechanisms

Thickness of composite plates plays an important role in the damage mechanism of single-pin-double-lap composite joints. As observed in Chapter 2 for woven glass-fabric/phenolic composite material as well as in Chapter 3 for glass/epoxy laminated composite materials, thickness variation would change local microscopic damage modes of joint structures. As shown in Chapter 2, for 1.96mm-thick (8-ply) composite plate, outward buckling of plies in composite plates accounts for the local bearing damage; for 5.97mm and 9.40mm-thick (24-ply and 40-ply) cases, however, kinky bands through the composite plate cross-section accounts for the local damage; for 20.42mm-thick (80-ply) case, local damage occurs when non-uniform kink bands develops through composite thickness with a concentration in outer plies. As shown in Chapter 3 about glass/epoxy composite joints, meanwhile, for 3.30mm and 6.48mm-thick (9-ply and 17-ply) composite plates, zig-zag kink bands account for the local bearing damage; whereas for 12.95mm-thick (34-ply) composite plate, net-section is the main damage when only few fiber kinks were found in the 0^{o}-plies close to the laminate surfaces in the bearing plane.

As shown in Chapter 2 and Chapter 3, large thickness, along with two other factors - adequate bonding between ply-interfaces and clamping force from bolting technique, provides a constraint in the thickness direction for the joint structure. In a local area beneath the pin where bearing damage usually occurs, this very constraint prevents fibers from buckling and composites from delamination at early stages of loading process.

Hence, increase in the first peak load capability is tangible, though limited, for joint structure with adequate constraint in the thickness direction.

With regard to ultimate damage load, or second peak load, and energy absorption during the damage process, however, constraint in the thickness direction, including large thickness, does not necessarily contribute positively. In fact, as observed in Chapter 3 for glass/fiber composite joint, higher constraints in the thickness direction result in more brittleness of joint load-displacement relationship, lowering the energy absorption in the damage process.

B. H/D ratio, load-displacement curve and stress distribution

As an important contribution initially recognized by Liu [13], H/D, i.e. geometric ratio of laminate thick to hole diameter, H/D, is found to be influential to joint mechanical performance in many respects. In fact, this concept was further explored in Chapter 2 and Chapter 4. In Chapter 2, the type of load-displacement curve of a joint was found to be dependent on the H/D ratio. Specifically, all the joints in the groups with H/D=0.4 and H/D=0.75 had brittle-type curves while all the joints in the group of H/D=1.5 had ductile-type curves. Meanwhile, pin-bending associated failure mechanism occurred in high H/D groups while composite bearing associated failure mechanism occurred in low H/D groups. Moreover, the group featuring H/D=0.75, being more close to 1 than other two groups with H/D=0.4 and H/D=1.5 respectively, seems to have more efficient load capability in terms of strength after comparison. These findings further reinforce the statement that H/D ratio is an important parameter in an efficient joint design.

As numerically discussed in Chapter 4, higher H/D would ensure higher stress concentration in plies close to composite outer surface. Based on failure criteria as included in Chapter 4, for high H/D joints, localized damage would occur at outer plies by local kink bands or outward buckling demonstrated in Chapter 2 and 3, coupling with pin bending as demonstrated in Chapter 2, and lead into a ductile-type load-displacement curve.

C. Size scaling

As explored in Chapter 2 and Chapter 3, three-dimensional size scaling in a composite joint structure is complicated. With respect to load capability, size scaling effect seems able to be separated into in-plane scaling effect and thickness scaling effect, as discussed in Chapter 2. For in-plane scaling, the bearing strength decreased as size increased; for thickness scaling, however, the bearing strength increased as thickness increased. Three-dimensional size scaling seems to be a complicated combination of in-plane scaling and thickness scaling, where bearing strengths either decreased monotonically or non-monotonically in different groups categorized by H/D ratio. Discussion in Chapter 3 further revealed that not only strength capability decreased monotonically, but also major failure mechanism shifted from bearing failure into net-section failure as joint size three-dimensionally scaled two and four times. All these findings demonstrated that three-dimensional size scaling needs to be carefully studied before results from small coupons could be used in order to predict joint performance in real application.

D. Investigation technique

As an important tool in understanding failure mechanisms, a finite element simulation of joint loading phenomenon, as demonstrated in Chapter 4, is crucial yet challenging task. Detailed three-dimensional stress study is time-consuming, even for modern computers and FEA programs. Nevertheless, study results included in Chapter 4 are much needed in a future failure investigation. The proposed two-parameter failure theory using thickness as characteristic dimension is inspiring and seems to make more physical sense. However, it needed to be tested and justified in a wider application.

5.2 Recommendations

In summary, the current study, using both experimental and analytical methods, demonstrated the complexity triggered by the thickness variation involved in a composite joint structure. Nevertheless, there are still many related areas uncovered by the scope of the current study. As a matter of fact, extensive further research would be needed in order to expand our knowledge and lead into an optimum composite joint design involving thickness requirement.

Possible recommendations for future study:

1. Material property variation caused by three-dimensional size scaling should be quantified by extensive material testing and the results should be integrated in a FEA model to correlate the strength variation observed in experimental studies.

2. Interface interaction from bonding technique as well as clamping force from bolting technique should be adequately integrated in a three-dimensional FEA in order to compare various thickness scaling techniques and guide an optimum composite joint design involving thickness requirement.

References

[1] Rajapakse Y. D. S. ed. Mechanics of Thick Composites, AMD Vol. 162. The American Society of Mechanical Engineers, 1993.

[2] Michaud D. J., Beris A. N. And Dhurjati P. S., "Curing Behavior of Thick-Sectioned RTM Composites", Journal of Composite Materials, Vol. 32, No. 14,1998. pp. 1273-1296.

[3] Chang, F. K., Perez, J. L. and Chang, K. Y., "Analysis of Thick Laminated Composites", Journal of Composite Materials, Vol. 24, 1990. pp801-822.

[4] Ayorinde E. O., "Elastic Constants of Thick Orthotropic Composite Plates", Journal of Composite Materials, Vol. 29, No. 8, 1995. pp.1025-1039.

[5] Frederiksen P. S., "Experimental Procedure and Results for the Identification of Elastic Constants of Thick Orthotropic Plates", Journal of Composite Materials, Vol. 31, No. 4, 1997. pp. 360-382.

[6] Hsial H. M., Danial I. M. and Wooh S. C., "A New Compression Test Method for Thick Composites", Journal of Composite Materials, Vol, 29, No. 13, 1995. pp. 1789-1806.

[7] Penn L. S., Jump J. R., Greenfield M. J. and Blandford G. E., "Use of the Free Vibration Spectrum to Detect Delamination in Thick Composites", Journal of Composite Materials, Vol. 33, No. 1, 1999. pp. 54-72.

[8] Her S. C., "Stress analysis of adhesively-bonded lap joints", Composite Structures, Vol. 47, Iss. 1-4, 1999. pp. 673-678.

[9] Tsai M. Y., Morton J. and Matthews F. L., "Experimental and Numerical Studies of a Laminated Composite Single-Lap Adhesive Joint", Journal of Composite Materials, Vol. 29, No. 9, 1995. pp. 1254-1277.

[10] Yeh M. K. and You Y. L., "Buckling of Laminated Plates with Adhesive Joints", Journal of Composite Materials, Vol. 29, No. 12, 1995. pp. 1565-1580.

[11] Adams R. D., Atkins R. W., Harris J. A. and Kinloch A. J., "Stress analysis and failure properties of carbon-fibre-reinforced-plastic/steel double-lap joints", J. Adhesion, Vol. 20, 1986. pp. 29-53.

[12] Bahei-El-Din Y. A. And Dvorak G. J., "New designs of adhesive joints for thick composite laminates", Composites Science and Technology, Vol. 61, No. 1, 2001. pp. 19-40.

[13] Dvorak G.J., Zhang J., Canyurt O., "Adhesive tongue-and-groove joints for thick composite laminates", Composites Science and Technology, Vol. 61, Iss. 8,2001. pp. 1123-1142.

[14] Bazant Z. P., "Scaling Laws in Mechanics of Failure", Journal of Engineering Mechanics, vol. 119, No. 9, 1993. pp. 1828-1844.

[15] Bazant Z. P., "Scaling Theories for quasi-brittle fracture: recent advances and new directions", Fracture mechanics of concrete structures, Proceedings of International Conference on Fracture Mechanics of Concrete Structures (2nd: 1995: Zurich: Switzerland). pp. 515-534.

[16] Bazant Z. P., Daniel I. M. and Li Z. Z., "Size Effect and Fracture Characteristics of Composite Laminates", Journal of Engineering Materials and Technology, Vol. 118, 1996. pp. 317-324.

[17] Gurvich M. R. and Byron P. R., "Strength Size Effect of Laminated Composites", Composite Science and Technology, Vol. 55, 1995. pp93-105.

[18] Jackson K. E., Kellas S. and Morton J., "Scale Effects in the Response and Failure of Fiber Reinforced Composite Laminates Loaded in Tension and in Flexure", Journal of Composite Materials, Vol. 26, No. 18, 1992. pp. 2674-2705.

[19] Wang H. S., Hung C. L. and Chang F. K., "Bearing Failure of Bolted Composite Joints. Part I: Experimental Characterization", Journal of Composite Materials, Vol. 30, No. 12, 1996. pp. 1284-1313.

[20] Park H.-J., "Effects of stacking sequence and clamping force on the bearing strengths of mechanically fastened joints in composite laminates", Composite Structures, Vol. 53, Iss. 2, 2001. pp. 213-221.

[21] Yi S. And Hilton H. H., "Effects of Thermo-Mechanical Properties of Composites on Viscosity, Temperature and Degree of Cure in Thick Thermosetting Composite Laminates during Curing Process", Journal of Composite Materials, Vol. 32, No. 7, 1998. pp. 600-622.

[22] Pillai V., Beris A. N. And Dhurjati P., "Intelligent Curing of Thick Composites Using a Knowledge-Based System", Journal of Composite Materials, Vol. 31, No. 1, 1997. pp. 22-51.

[23] Gascoigne H. E., "Residual Surface Stresses in Laminated Cross-ply Fiber-epoxy Composite Materials", Experimental Mechanics, Vol. 51, 1994. pp. 27-36.

[24] Joh D., Byun K. Y. and Ha J., "Thermal Residual Stresses in Thick Graphite/Epoxy Composite Laminates-Uniaxial Approach", Experimental Mechanics, Vol. 50, 1993. pp. 70-76.

[25] Oplinger D. W., "Bolted Joints in Composite Structures – An Overview", AGARD conference proceedings 590, 83rd, Jan., 1997; 1-1—1-12.

[26] Nelson W. D., Bunin B. L. and Hart-Smith L. J., "Critical Joints in Large Composite Aircraft Structure", Proceedings of the Sixth Conference on Fibrous Composites in

Structural Design, pp II-2 to II-38, Army Materials and Mechanics Research Center Manuscript Report AMMRC MS 83-2.

[27] Ireman T., "Three-dimensional stress analysis of bolted single-lap composiite joints", Composite Structures, Vol. 43, 1998. pp. 195-216.

[28] Liu D., Raju B. B., You J. L., "Thickness Effects on Pinned Joints for Composites", Journal of Composite Materials, Vol. 33, 1999. pp. 2-21.

[29] Spering U. O., "Three-dimensional Stress Distribution Around Pin Loaded Holes in Composite Laminates", AIAA Proceedings, 85-0826, 1985. pp. 743-750.

[30] Chen W. H., Lee S. S. and Yeh J. T., "Three-dimensional contact stress analysis of a composite laminate with bolted joint", Composite Structures, Vol. 30, 1995. pp. 287-297.

[31] Iarve E. V., Schaff J. R., "Stress analysis of open and fastener hole composite based on three dimensional spline variational technique", AGARD Conference Proceedings No. 590, Florence, Italy, 2-3 September, 1996.

[32] Shokrieh M. M. and Lessard L. B., "Effects of Material Nonlinearity on the Three-Dimensional Stress State of Pin-Loaded Composite Laminates", Journal of Composite Materials, Vol. 30, No. 7, 1996. pp. 839-861.

[33] Waszczak J. P. and Cruse T. A., "Failure mode and strength prediction of anisotropic bolt bearing specimens", Journal of Composite Materials, No.5, 1971. pp. 421-425.

[34] Tang S., "Failure of composite joints under combined tension and bolt loads", Journal of Composite Materials, No. 15, 1981. pp. 329-335.

[35] Crews J. H. and Naik R. A., "Combined bearing-bypass loading on a graphite/epoxy laminate", Composite Structures, No. 6, 1986. pp. 21-40.

[36] Naik R. A. and Crews J. H., "Ply-level failure analysis of a graphite/epoxy laminate under bearing-bypass loading", NASA Tech. Memo. 100578, 1988. pp. 1-35.

[37] Hart-Smith, L. J., "Mechanically-fastened joints for advanced composites-phenomelogical considerations and simple analysis", Douglas Paper 6748, 1978. pp. 1-32.

[38] Whitney J. M. and Nuismer R. J., "Stress fracture criteria for laminated composites containing stress concentrations", Journal of Composite Materials, No. 8, 1974. pp. 253-265.

[39] Nuismer R. J. and Labor J. D., "Applications of the average stress failure criterion: part I-tension", Journal of Composite Materials, No. 12, 1978. pp. 238-249.

[40] Nuismer R. J. and Labor J. D., "Applications of the average stress failure criterion: part II-compression", Journal of Composite Materials, No. 13, 1979. pp. 49-60.

[41] Agarwal B. L., "Static strength prediction of bolted joint in composite materials", AIAA J., No. 18, 1980, pp. 1371-1375.

[42] Chang F. K., Scott R. A. and Springer G. S., "Strength of mechanically fastened composite joints", Journal of Composite Materials, No. 16, 1982. pp. 470-494.

[43] Hashin Z., "Failure criteria for unidirectional fiber composites", Journal of Applied Mechanics, No. 47, 1980. pp. 329-334.

[44] Chang F. K. and Chang K. Y., "A progressive damage model for laminated composites containing stress concentrations", Journal of Composite Materials, No. 21, 1987. pp. 834-855.

[45] Chen W. H. and Lee Y. J., "Failure process and pin-bearing strength of laminated composites at elevated temperatures", Journal of Plastics and Composites, No. 11, 1992. pp.743-771.

[46] Chen W. H. and Lee S. S., "Numerical and experimental failure analysis of composite laminates with bolted joints under bending loads", Journal of Composite Materials, No. 29, 1995. pp. 15-36.

[47] Lessard L. B. and Shokrieh M. M., "Two-dimensional modeling of composite pinned-joint failure", Journal of Composite Materials, No. 29, 1995. pp. 671-697.

[48] Chang F. K. and Lessard L. B., "Damage tolerance of laminated composites containing an open hole and subjected to compressive loadings: part 1-analysis", Journal of Composite Materials, No. 25, 1991. pp. 2-43.

[49] Chang K.Y., Liu S. and Chang F. K., "Damage tolerance of laminated composites containing an open hole and subjected to tensile loadings", Journal of Composite Materials, No. 25, 1991. pp. 274-301.

[50] Tsai S. W. and Hahn H. T., "Introduction to Composite Materials", Technomic Publishing Company, Westport, 1980.

[51] Chang F. K. and Chang K. Y., "Post-failure analysis of bolted composite joints in tension or shear-out mode failure", Journal of Composite Materials, No. 21, 1987. pp. 809-833.

[52] Chang F. K., Scott R. A. and Springer G. S., "Failure strength of nonlinearly elastic composite laminates containing a pin loaded hole", Journal of Composite Materials, No. 18, 1984. pp. 464-477.

[53] Tan S.C., "A progressive failure model for composite laminates containing openings", Journal of Composite Materials, No. 25, 1991. pp. 556-557.

[54] Marcia P.-M., Patrick J. P. and Frederick W. S., "Modeling Bolted Connections in Wood: Review", Journal of Structural Engineering, vol. 123, No. 8, 1997. pp. 1054-1062.

[55] Hung C. L. and Chang F. K., "Bearing Failure of Bolted Composite Joints. Part II: Model and Verification", Journal of Composite Materials, Vol. 30, No. 12, 1996. pp. 1359-1400.

[56] Stockdale J. H. and Matthews F. L., "The effect of clamping pressure on bolt bearing loads in glass fibre-reinforced plastics", Composites, January, 1976. pp. 35-38.

[57] Kollegal M. G., Sridharan S., "Compressive Behavior of Plain Weave Lamina", Journal of Composite Materials, Vol. 32, No. 15, 1998. pp. 1334-1355.

[58] Naik R. A., "Failure Analysis of Woven and Braided Fabric Reinforced Composites", Journal of Composite Materials, Vol. 29, No. 17, 1995. pp. 2334-2365.

[59] Oguni K., Tan C. Y. and Ravichandran G., "Failure Mode Transition in Unidirectional E-Glass/Vinylester Composites under Multiaxial Compression", Journal of Composite Materials, Vol. 34, No. 24, 2000. pp. 2081-2097.

[60] Marshall I. H., Arnold W. S., Wood J. and Monsley R. F., "Observations on bolted connections in composite structures", Composite Structures, Vol. 13, 1989. pp. 133-151.

[61] Lee Y. J. and Chen W. H., "Study on the failure behavior of bolted connections in vessel made of GFRP laminates", J. Soc. Naval Architects of Japan, 169, 1991. pp. 467-476.

[62] Hoyle G. and Ineson E., J. Iron Steel, Inst., 191, 44, 1959.

[63] Grobe A. H. and Roberts G. A., Transactions of the American Society of Metals, 40, 435, 1948.

[64] Zhang G., Robert A. L., JR., "The Prevention of Kind Band Formation at Free Edges of Unidirecitional Composite under Compressive Load", Journal of Composite Materials, Vol. 31, No. 24, 1997. pp. 2426-2443.

[65] Collings T. A., "On the bearing strengths of CFRP laminates", Composites, Vol. 13, 1982. pp. 241-252.

[66] Oh J. H., Kim Y. G., Lee D. G., "Optimum bolted joints for hybrid composite materials", Composite Structures, Vol. 38, 1997. pp. 329-341.

[67] Hart-Smith L. J., "Analysis Methods for Bolted Composite Joints Subjected to In-Plane Shear Loads", 83rd, Bolted/Bonded Joints in Polymeric Composites, AGARD Conference Proceedings 590, Jan. 1997.

[68] Oakeshott J.L., Gower M., Perinpanayagam S. and Matthews F.L., "Development of Failure in Bolted Joints in Woven CFRP Laminates", 83rd, Bolted/Bonded Joints in Polymeric Composites, AGARD Conference Proceedings 590, Jan. 1997.

[69] Ersoy N. and Vardar O., "Measurement of Residual Stresses in Layered Composites by Compliance Method", Journal of Composite Materials, Vol. 34, No. 7, 2000. pp. 575-598.

[70] Eriksson, L. I., "Contact stresses in bolted joints of composite laminates", Composite Structures., Vol. 6, 1986. pp. 57-75.

[71] Rahman M. U. And Rowlands R. E., "Finite element analysis of multiple bolted joints in orthotropic plates", Computers and Structures, Vol. 46, No. 15, 1993. pp. 859-867.

[72] Chiang Y. J. And Rowlands R. E., " Finite element analysis of mixed-mode fracture of bolted joints in composites ", Journal of Composites Technology and Research, Vol. 13, No. 4, 1991. pp.227-235.

[73] Kim S. J. And Kim J. H., "Finite element analysis of laminated composites with contact constraint by extended interior penalty methods ", International Journal for Numerical Methods in Engineering, Vol. 36, 1993. pp. 3421-3439.

[74] Pierron F., Cerisier F. and Grediac M., "A Numerical and Experimental Study of Woven Composite Pin-Joints ", Journal of Composite Materials, Vol. 34, No. 12, 2000. pp. 1028-1054.

[75] Hosur M. V., Alexander J., Uaidya U. K. and Jeelani S., "High strain rate compression response of carbon/epoxy laminate composites", Composite Structures, Vol 52, 2001. pp. 405-417.

[76] Wass A. M., Takeda N., Yuan J. and Lee S. H., "Static and dynamic compressive behavior of glass fiber reinforced unidirectional composites", Proceedings 12th Annual Technical American Society for Composites Conference, 6-8 October, 1997, Dearborn, pp. 552-561.

[77] Hsiao H. M., Daniel I. M. and Cordes R. D., "Strain rate effects on the transverse compression and shear behavior of unidirectional composites", Journal of Composite Materials, Vol. 33. No.17, 1999. pp. 1620-1642.

[78] Sierakowski R. L., "Strain rate effects in composites", Applied Mechanics Review, Part 1, Vol. 50, No. 11:741-61, 1997.

[79] Ger G. S., Kawata K. And Itabashi M., "Dynamic tensile strength of composite laminate joints fastened mechanically", Theoretical and Applied Fracture Mechanics, Vol. 24, 1996. pp. 147-155.

[80] Li Q. M., Mines R.A.W and Birch R.S., "Static and dynamic behaviour of composite riveted joints in tension", International Journal of Mechanical Sciences, Vol. 43, 2001. pp. 1591-1610.

[81] Hamada H., Maekawa Z. I. and Haruna K., "Strength Prediction of Mechanically Fastened Quasi-Isotropic Carbon/Epoxy Joints", Journal of Composite Materials, Vol. 30, No. 14, 1996. pp.1596-1611.

[82] Weibull W., "A statistical theory of strength of material", Proc. Royal Swedish Inst. Engng, 151, 1939.

[83] Liu D., Raju B.B. and Dang X., "Impact Perforation Resistance of Laminated and Assembled Composite Plates", International Journal of Impact Engineering, 24(6-7), 2000. pp. 733-746.

[84] Liu D., Shakour E. and Lu X., "Joining Forces in Assembled Composite Beams," Journal of Composite Materials, Vol. 35, No.22, 2001. pp.1985-2008.

[85] Kretsis G. and Matthews F.L., "The Strength of Bolted Joints in Glass-fibre/Epoxy Laminates", Composites, 16, 1985. pp. 92-105.

[86] Collings T.A., "The Strength of Bolted Joints in Multi-directional CFRP Laminates", Composites, 8, 1977. pp. 43-54.

[87] Matthews F.L., Kilty P.F. and Godwin. E.W., "Load-carrying Joints in Fibre Reinforced Plastics", Plastic and Rubber Process and Applications, 2, 1982. pp.19-25.

[88] Tsai, M. Y. and Morton, J., "Stress and Failure Analysis of a Pin-Loaded Composite Plate: An Experimental Study", Journal of Composite Materials, Vol. 24, 1990. pp.1101-1121.

[89] Blom A, Ansell H, Nyman T, Schon J., "Fatigue of composite airframe structures", Proceedings of the International Conference on Fatigue of Composites, Paris, 3-5 June, 1997.

[90] Tsai S. W., Strength theories of filamentary structures in Fundamental Aspects of Fiber Reinforced Plastic Composites, Schwartz, R. T. and Schwartz, H. S., Eds, Wiley Inter-science, New York, 1968, 3.

[91] Tsai S. W. and Wu E. M., "A general theory of strength for anisotropic materials", Journal of Composite Materials, No. 5, 1971. pp.58.

[92] Argon A. S., "Fracture of composites", Treatise Mater. Sci. Technol. 1, 1972. pp. 79-114.

[93] Budiansky, B., Micromechanics, Compt. Struct., 16, 1983. pp. 3-12.

[94] Yamada S.E. and Sun C.T., "Analysis of laminate strength and its distribution", Journal of Composite Materials, No. 12, 1978. pp. 275-284.

[95] Puck A., Festigkeitsanalyse von Faser-Matrix laminaten-Modelle fur die Praxis, Carl Hanser Verlag, 1995.